DVB-RCS2 Satellite Return Link: Queueing Model and Resource Allocation Optimization Based on Game Theory

Author: Pedro Henrique Andrade Trindade
Advisor: Dr. Leonardo Aguayo

Universidade de Brasília - UnB
Electrical engineering Department - PPGEE
M.S. in Electrical Engineering

Brasília, DF
2022

Pedro Henrique Andrade Trindade

DVB-RCS2 Satellite Return Link: Queueing Model and Resource Allocation Optimization Based on Game Theory

Enlace de Retorno Satelital DVB-RCS2: Modelagem de Fila e Otimização de Alocação de Recursos Baseada em Teoria dos Jogos

Dissertation submitted to the Electrical Engineering Department of University of Brasilia as a prerequisite to acquire the title of M.S. in Electrical Engineering.

Universidade de Brasília - UnB

Electrical Engineering Department - PPGEE

Advisor: Leonardo Aguayo

Brasília, DF

2022

Pedro Henrique Andrade Trindade

DVB-RCS2 Satellite Return Link: Queueing Model and Resource Allocation Optimization Based on Game Theory / Pedro Henrique Andrade Trindade. – Brasília, DF, 2022-

115 p; 30 cm. Número da Ficha Catalográfica 787/22

Advisor: Leonardo Aguayo

Master Dissertation – Universidade de Brasília - UnB
Electrical Engineering Department - PPGEE , 2022.

1. DVB-RCS2. 2. Game Theory. I. Leonardo Aguayo. II. Universidade de Brasília. III. Electrical Engineering Department. IV. DVB-RCS2 Satellite Return Link: Queueing Model and Resource Allocation Optimization Based on Game Theory

Enlace de Retorno Satelital DVB-RCS2: Modelagem de Fila e Otimização de Alocação de Recursos Baseada em Teoria dos Jogos

Pedro Henrique Andrade Trindade

DVB-RCS2 Satellite Return Link: Queueing Model and Resource Allocation Optimization Based on Game Theory

Dissertation submitted to the Electrical Engineering Department of University of Brasilia as a prerequisite to acquire the title of M.S. in Electrical Engineering.

Dissertation Approved. Brasília, DF, June 24 of 2022:

Leonardo Aguayo
Advisor

Vicente Angelo de Sousa Junior
Invited Professor 2

Marcelo Menezes de Carvalho
Invited Professor 1

Brasília, DF
2022

I dedicate this work to the worm that first gnawed at the cold flesh of my corpse, also my mom, brothers, my advisor and my friends (because not every cliché is a bad cliché, right?). They helped me get through this important path without any permanent damage.

I also dedicate this work as a personal requiem to the millions of COVID-19 victims that had their lifes taken away too early by our human limitations and flaws.

ACKNOWLEDGEMENTS

I want to thank the University of Brasilia (UnB), CAPES and third-party telecommunication companies that financed this project and provided the opportunity for it to be developed. A very special recognition to my advisor, Prof. Dr. Leonardo Aguayo, from which the immeasurable wisdom adjoined with his unique, fluid, and fruitful project/research managing skills allowed me to develop autonomy to originate and to answer my own research questions in a very encouraging manner, helping me to develop both as a person and as a professional.

This dissertation would not have been possible without the inestimable aid of Prof. Dr. Alexander Wyglinski, Professor of Electrical Engineering and Robotics Engineering at Worcester Polytechnic Institute (WPI), who along with his graduate student Dr. Renato Iida, worked on the programming of the satellite simulator, continuously maturing, expanding, and evolving our understanding of the paradigm we performed over and the solutions to the engineering problems that emerged from its demands.

It is also important to display an unprecedented gratitude towards the professors of the Electrical Engineering and Mathematics departments of UnB, for all the ones that made the extra effort to, even in these trying times of pandemics, teach the essential courses with mastery and such *joie-de-vivre* to inspire the potential new generation of researchers with the beautiful and important aspects of blossoming knowledge through the scientific methodology, also serving as a colossal example to be followed, in contrast to the professors that can learn from this impetus.

And last but not least, from a personal side, i want to thank my family and friends, specially my mom Angelica Trindade, which was the foundation pillar of my flourishing as a human being, ultimately leading me to this point. Giving me the endmost hope as to why keep doing my best at every opportunity, expecting to reach a better place for me and those around me.

“I have this thing about being acknowledged and accepted by institutions.“

- Mitski.

Resumo

É esperado que satélites tenham um papel fundamental no futuro dos sistemas de comunicação, integrando-se às infraestruturas terrestres. Esta dissertação de mestrado propõe três contribuições principais: primeiramente, se apresenta um arcabouço de simulação capaz de prover detalhes da performance de redes de comunicação satelital em cenários realistas. Este arcabouço aplica uma metodologia orientada a eventos, modelando a rede de comunicação como um sistema baseado em eventos discretos (DES), focando no enlace de retorno do protocolo DVB-RCS2. Três diferentes cenários simulados demonstram os possíveis usos das saídas do simulador para entender o comportamento dinâmico da rede e alcançar um ponto ótimo de operação do sistema. Cada cenário explora uma característica diferente do simulador, enquanto cobre um grande território de usuários, que em nosso caso estudo o país de escolha foi o Brasil. Em um segundo tópico, este trabalho introduz um novo algoritmo modificado do método de alocação de *timeslots* baseado em teoria dos jogos, aplicando-se no protocolo DVB-RCS2. Este procedimento considera a eficiência espectral do terminal como um parâmetro de peso para o problema de otimização convexa resultante da solução da barganha de Nash. Este novo método garante o cumprimento dos requisitos de Qualidade de Serviço (QoS) enquanto provê uma medida de justiça maior; os resultados mostram uma melhoria de 5% na medida de justiça, com uma diminuição de 75% no desvio padrão de justiça entre os quadros, também alcançando um aumento de 12% na satisfação individual média pela alocação de capacidade aos terminais. Por final, apresentamos uma modelagem alternativa para o enlace de retorno do DVB-RCS2 usando cadeias de Markov, predizendo parâmetros tradicionais de fila como a intensidade de tráfego, tempo médio de espera, dentre outros. Utilizamos dados coletados de uma série de simulações usando o arcabouço orientado a eventos para validar o modelo de filas como uma aproximação numérica útil para o cenário real de aplicação. Nós apresentamos o algoritmo de alocação de controle do parâmetro alfa (GTAC) que consegue controlar o tempo médio de espera de um RCST na fila, respeitando um limiar de tempo enquanto otimiza a taxa média média de transmissão de dados dos terminais.

Palavras-chave: DVB-RCS2, Comunicação por Satélite, Teoria dos Jogos, Solução do problema da barganha de Nash, Otimização do quadro MF-TDMA, Modelagem de filas, Simulação orientada a eventos.

Abstract

Satellite networks are expected to play a vital role in future communication systems, with complex features and seamless integration with ground-based infrastructure. This dissertation proposes three main contributions: firstly, it presents a novel simulation framework capable of providing a detailed assessment of a satellite communication's network performance in realistic scenarios, employing an event-driven methodology and modeling the communications network as a DES (discrete event system). This work focuses on the return link of the Digital Video Broadcast Return Channel via Satellite (DVB-RCS2) standard. Three different scenarios demonstrate possible uses of the simulator's output to understand the network's dynamic behavior and achievable optimal system operation. Each scenario explores a different feature of the simulator. The simulated range covers a large territory with thousands of users, which in our case study was the country of Brazil. In the second theme, this work introduces a novel algorithm modification for the conventional game theory-based time slot assignment method, applying it to the DVB-RCS system. This procedure considers the spectral efficiency as a weighting parameter. We use it as an input for the resulting convex optimization problem of the Nash Bargaining Solution. This approach guarantees the fulfillment of Quality of Service (QoS) constraints while maintaining a higher fairness measure; results show a 5% improvement in fairness, with a 73% decrease in the standard deviation of fairness between frames, while also managing to reach a 12.5% increase in average normalized terminal BTU allocation satisfaction. Lastly, we present an alternative queuing model analysis for the DVB-RCS2 return link using Markov chains, developed to predict traditional queue parameters such as traffic intensity, average queue size, average waiting time, among others. We used data gathered from a series of simulations using the DES framework to validate this queuing model as a useful numerical approximation to the real application scenario, and, by the end of the scope, we present the alpha allocation algorithm (GTAC) that can maintain the average waiting time of a terminal in the queue to a threshold while optimizing the average terminal throughput.

Keywords: DVB-RCS2, Satellite Communications, Game Theory, Nash Bargaining Solution, MF-TDMA Optimization, Queue Modelling, Event-Driven Simulation.

List of Figures

List of Tables

LIST OF ABBREVIATIONS AND ACRONYMS

ACM	Adaptive Coding and Modulation
BoD	Bandwidth on Demand
BTU	Bandwidth/Time Unit
CAPEX	Capital Expenditure
CRA	Constant Rate Assignment
DA	Dedicated Access
DAMA	Demand Assigned Multiple Access
DES	Discrete Event Simulation
DRA	Dynamic Rate Adaption Channel
DVB-RCS2	Digital Video Broadcast Return Channel Second generation Standard
DVB-S2X	Digital Video Broadcast Satellite Second Generation Extended
ETSI	European Telecommunications Standards Institute
FCA	Free Capacity Assignment
GEO	Geostationary orbit
ITU	International Telecommunication Union
KPI	Key Performance Indicators
LEO	Low Earth Orbit
M2M	Machine to Machine communication
MAC	Medium Access Control Layer
MEO	Medium Earth Orbit

MF-TDMA Multi Frequency Time Division Multiple Acess

MODCOD Modulation and Codification schemes

NCC Network Control Center

OPEX Operational Expenditure

PHY Physical Layer

PLR Packet Loss Rate

QoS Quality of Service

RRM Radio Resource Management

RA Random Access

RACH Random Access Channel

RBDC Rate Based Dynamic Capacity

RCST Return Channel Satellite Terminal

SF SuperFrame

SLA Service Level Agreement

SNIR Signal to Noise and Interference Ratio

SNR Signal to Noise Ratio

TBTP Terminal Burst Time Plan Table

TS Timeslot

TTC Tracking, Telemetry and Control

UHDTV Ultra High Definition TV

VBDC Volume-Based Dynamic Capacity

LIST OF SYMBOLS

λ	Average number of RCSTs arrivals per SF
ρ	Traffic intensity
B_L	Buffer length
P_q	Probability of a terminal waiting in the queue
N_Q	Average number of terminals waiting in the queue
N_d	Number of simulation drops
V_i	Volume of data for an RCST to transmit
$\mathbb{Z}$	The set of integers
$\mathbb{R}$	The set of real numbers
μ	Average service rate in the queue
m	Predicted capacity of RCSTs allocation in a SuperFrame
β	Normalizing constant of the truncated Poisson distribution.
ϕ_i	Number of BTUs allocated to RCST i
υ	Convex solution's constraint constant
$\mathcal{N}_B$	Nash Bargaining problem objective function
$\mathcal{L}(\boldsymbol{\phi})$	Lagrangian of the BTU distribution to each RCST
$\boldsymbol{\pi}$	Stationary probability vector
E_s/N_0	Signal-to-noise ratio
d_i	i-th RCST's minimum required data rate
D_i	i-th RCST's requested data rate
η_i	i-th RCST's spectral efficiency

p_i	i-th RCST's allocation priority
q_i	Effective information per BTU
a_i	Probability of i RCSTs arrivals in a SuperFrame
$P_C^k(i)$	Probability of i RCSTs completions given Markov state k
ω_i	i-th RCST's burst length in BTUs
N_{SF}	Number of BTUs in a SuperFrame
T_{SF}	Time in BTUs of a SuperFrame
K_{SF}	Number of DRAs in a SuperFrame
T_{sim}	Simulation time in SuperFrames
T_{th}	Maximum waiting time threshold
$N_{U,t}$	Expected number of users in the network at time t.
R_i	Agreed data rate.
P_i	Payload in the i-th RCST's ACM.
α	Allocation ratio between D_i and d_i
$J(\phi)$	Jain's fairness index
κ, k_i and K_i	Lagrange Multipliers

Contents

CHAPTER 1

INTRODUCTION

1.1 First Considerations

The current percentage of the worldwide population with Internet access is nearly 60%, which is unequally distributed between developed and developing countries. According to ITU-D statistics [1], the global availability of Internet access in 2019 per 100 users varied from 90% for developed countries to 20% for nations on the UN list of Least Developed Countries (LDCs), where poor social and economic development are the primary factors that limit ubiquitous and affordable Internet. In several countries, large territorial extension and geographic obstructions, such as mountains or dense forests, prevent the deployment of conventional cellular or cabled-based infrastructure.

Beyond the necessity to provide sufficient Internet access to the population, the recent increase in Machine-to-Machine (M2M) traffic, resulting from 5G/6G and IoT networks, imposes new challenges for service providers. Current estimates predict that the number of devices connected to the Internet within five years will be approximately 25 billion [2], which further emphasizes the urgency for efficient utilization of radio resources and its integration among different Radio Access Technologies. This scenario is a challenging environment for network deployment and operation, not only in terms of Capital Expenditure (CAPEX) and Operating Expenses (OPEX) management, but also in the realms of initial network planning, heterogeneous traffic demand management, and coexistence with legacy infrastructure.

As an alternative telecommunication technology that can potentially serve inaccessible regions of the world, satellites can provide extended coverage for terrestrial networks and perform traffic offloading. Access to satellite communications can operate independently of ground-based cellular infrastructure, but the convergence trend to an IP-based service platform requires new approaches for combined planning and the operation of ground and space segments. Although challenges associated with the integration of cellular and satellite networks can be traced back to 2G GSM systems [3], recent studies [4] address new interoperability challenges

and joint Radio Resource Management (RRM) strategies for 5G and 6G network architectures.

For complex communication systems, the accurate inference of a network's performance requires system-level simulations, typically due to the difficulty of obtaining analytical solutions that consider all details related to protocol specifications and user behavior. Furthermore, the effect of complex relationships among the system's configuration parameters and the corresponding network operations can be better understood through a careful design of simulation scenarios. A controlled environment may stress the relevance of specific parameters that: (i) are not directly accessible by the network management system, or (ii) are out of the scope of a control system operated by the service provider. Planning and operations activities may use system-level simulations as a tool for potential savings on CAPEX and OPEX. Finally, representatives in standardization forums often use system-level simulations to address open issues, improve recommendations, and propose new features for the network nodes.

Satellite networks are expected to play a vital role in 5G and beyond communications systems, especially in the context of hybrid terrestrial-satellite networks. Optimization of radio resources in the uplink is fundamental to coping with data rate requirements within a machine-to-machine (M2M) scenario. The ETSI Digital Video Broadcasting-Satellite (DVB-S) standard presents advances for the forward link with DVB-S2X [5] via new modulation and coding (MODCOD) schemes with high spectral efficiency. For the return link, DVB-RCS2 [6, 7] offers an advanced and flexible configuration for multiuser access Multi-Frequency Time Division Multiple Access (MF-TDMA) framework. This work addresses the optimization of multiuser allocation in the MF-TDMA structure considering different user priorities and the MODCOD options allowed by the RCS2 standard.

1.2 Objectives

This dissertation started as a demand for a major development project to a large fleet tracking company in Brazil. The objective was to develop a systemic simulator for the DVB-S2X/DVB-RCS2 satellite communication system, focusing on the realism of its implementation, with the goal of enabling system dimensioning and Quality of Service (QoS) predictions for its large customer base. At the beginning, the project aimed to develop an alternative framework for the commonly used NS-3 network simulator, an idea that allowed the development of a new Discrete Event Simulation framework for the systemic analysis of the DVB uplink. After the

validation of the results in basic resource allocation algorithms, the system evolved, allowing the exploration of the state of the art of scheduling performance.

Given this background, we underline the scope of this dissertation as the study, modeling, implementation, and optimization of the scheduling scheme of the DVB-RCS2 standard return link, focusing on the application of fleet tracking. This particular application is generalized when not specified otherwise within the text. Academically, the study and optimization of the DVB-RCS2 uplink resource allocation system is motivated by a number of different research papers and related work, which we describe next.

1.3 Related Work

On the simulation of recent wireless systems, Ying Wang et al. [8] describe challenges for simulating 5G networks. In the context of Wireless Sensor Networks (WSNs), a review of simulation tools can be found in the work of Anand Nayyar et al. [9] and its references. Regarding the simulation of satellite communications, D.P. Connors et al. [10] describes modeling aspects for the medium access control (MAC) layer. More recently, ns-3 was used as the base framework engine to build a detailed implementation of RCS2 [11] [12].

With a focus on the optimization of radio resources in DVB-RCS2, Dong-Hyun Jung et al. [13] present an algorithm for the DVB-RCS2 superframe design and user allocation based on Jain's fairness index, but it does not explicitly mention the system performance in terms of capacity. In J. R. Bejarano et al . [14], the authors consider MF-TDMA allocation in a multi-spot scenario for Very High Throughput Satellites, but do not provide any details related to the MAC layer being employed as the logon phase and using random access channels. A MAC procedure using Successive Interference Cancellation (SIC) with direct application to the MF-TDMA structure of RCS2 (CRDSA) can be found in E. Casini et al. [15]. The paper of Pietrabissa et al. [16] define an algorithm created to optimize RCS2 radio resources; in this work, simulations were performed with few terminals and within a spatial range of 250 km.

In general, an event-driven simulation framework can be implemented in different ways and programming languages. The SimEvents framework [17] uses the Simulink and Matlab, and it has been used in connected vehicle communications [18]. The framework presented in this dissertation employs a fusion of a static simulation used in standardization contributions [19] and the event-driven library SimPy [20].

On the resource allocation problem and scheduling, as explained thoroughly

by J.B. Dupé [21], there are three main categories of analytic frameworks for defining scheduling criteria: The scheduling algorithms based on empirical/explicit criteria, algorithms based on game theory, and algorithms that expand the use of utility functions beyond the scope of game theory to define its resource allocation policies.

Different approaches were considered to optimize the MF-TDMA resource allocation in DVB-S systems, such as optimizing power allocation in multi-beam satellites [22]. Antoni Morell et al. [23] and Gonzalo Seco-Granados et al.[24] present a game-theoretic approach to solving the Nash bargaining problem with Lagrange multipliers. T. Zhang et al. [25] employ a buddy-fit algorithm and S. Alouf et al. [26] propose an algorithm to analyze the spatial constraints and interference patterns in the satellite configuration.

This work relies on a different approach on the game-theoretic solution, implementing the Nash bargaining solution described in Antoni Morell et al. [23] using the Return Channel Satellite Terminal's (RCSTs) SNIR as a weighting parameter. This strategy as implemented as the SNIR defines the terminal Modulation and Coding Schemes (MODCOD) and thus, its information payload. This strategy leads to a means to prioritize the resource distribution in the dimensions of the SuperFrame (SF), concerned not only with the minimum requirements of QoS but also fairness.

In our context, we are representing the MF-TDMA frame as a queueing system, working with a discrete time multi-server queue where the number of servers m is a random variable. It represents the number of RCSTs served at a given frame and it depends on the RCST pool. This value m has emerging statistical properties and can be approximated. We use this fact to predict metrics of the queue system. Li Hui and Tao Yang [27] tackle a similar problem of a multi-server queue with variable number of serves for computer communication networks, but not in the context of a MF-TDMA frame.

The queue and dynamic scheduling literature is vast, the problem of analyzing the discrete-time multi-server queue was explored in different papers [28, 29, 30], but an explicit analytical solution to the queue we are defining for the DVB-RCS2 uplink can be quite challenging to be found in closed form, so we decided to implement a Markov chain model approximation. We use DVB-S2X standard-compliant simulated data to improve the numerical results.

1.4 Research Questions

As far as literature review goes, the guiding principle to our research was the pragmatic approach of obtaining a simulator for a DVB standard compliant scenario.

This approach leads us to the most frequent implementation frameworks, scheduling algorithms and models used in this sort of environment. After the extensive process of code development and literature study, we realized some main possibilities as to where the system could be optimized, guided by some initial questions:

Question 1 (Q1): What are the variables and trade-offs that affect the DVB-RCS2 return link resource allocation algorithms?

Question 2 (Q2): Can the Nash bargaining resource allocation algorithm be optimized? What can be said about fairness in this scheduling context?

Question 3 (Q3): Can the DVB-RCS2 scheduling scheme be modeled as a queueing model? Can we make predictions over its systemic behavior *a priori* of numerical simulation?

These three main questions occupied the utmost part of this research scope, and *a posteriori* from unraveling them, two additional questions were added, for closure purposes, to this catalog:

Question 4 (Q4): What can be implied from our experiments and what previous hypothesis are supported by it?

Question 5 (Q5): What are the possible directions that the study of the DVB-RCS2 return link scheduling can take in the future?

We intend to discuss these five questions in a convincingly manner until the end of the dissertation, giving the reader the technical background to grasp the justification for our design decisions and their consequences.

1.5 Dissertation Outline

To summarize the contents of this work, we describe its chapters to highlight the line of reasoning conducted by them, as each division sheds light on a different aspect of the dissertation construction, being contiguous and accumulative to the conclusions.

Chapter 2: Satellite Communications

In this chapter, we describe the necessary background to understand the system overview; the fundamental pieces of the DVB-RCS2 inner workings; its compo-

nents; and the definitions of the DVB guidelines. We also explain the DVB capacity request/BoD framework in depth, which is used in later chapters as the basis for the scheduling algorithms. Finally, we discuss the general satellite telecommunications context in our current time, how the technology has evolved until this point, what aspects of this category of networks stand out in a commercial setting, and the importance of this dissertation's study topic.

Chapter 3: Theory Overview

In this chapter, we delve into this dissertation's main topics: first, we summarize the game theory mathematical branch, outline its objectives, and describe the bargaining problem formulation. In addition, we present the Nash Bargaining Solution and its axiomatic approach. Secondly, we briefly review basic queueing and probability theory in order to detail the performance metrics used in later sections. Finally, we provide a short overview of Discrete-Event Simulations (DES) systems, which serve as the cornerstone for our developed solution.

Chapter 4: Proposed System and Methodology

Here lies the majority of the contribution; we detail the mathematical modeling of the three main contribution fronts: firstly, to describe the inner workings of the Python simulator constructed; secondly, the resource allocation algorithms used to validate the simulator; and finally, a description of the Nash Bargaining convex problem formulation. We explain all the implementation details and the relevant choices for proper integration with the simulator. We aim to demonstrate the improvement of our proposed algorithm in fairness and in average allocation satisfaction. We describe the mathematical formulation and the arguments for defining an interpretation of the MF-TDMA return link allocation system as a queue system. With this interpretation, we define metrics that are analogous to the multi-server discrete-time queue and use similar tools to predict the behavior of the DVB resource allocation scheme. Using these main features of our work, we developed a resource allocation algorithm called Game Theory Alpha Control Allocation (GTAC) that can keep the average time-until-served of the whole system below a threshold while maximizing average throughput of each terminal.

Chapter 5: System Performance

This is the chapter where we validate our hypothesis and design choices from the previous chapter. We analyze carefully the results presented, which were carefully chosen among dozens of other results the designed simulator produces, specifically to cover the scope of this work's experiments. We list all of the simulation parameters for reproducibility purposes, which means that any result shown in this dissertation

can be further scrutinized, re-validated, and improved upon in future works.

Chapter 6: Conclusion and Future Work

This chapter is dedicated to explaining the implications of the work here developed, trying to encapsulate the information encompassed by the ensemble of experiments accomplished. Furthermore, we discuss potential future directions for research in this theme in order to improve the findings in this dissertation.

1.6 Dissertation Contributions

Here we present the two publications that we achieved in the period of this dissertation development:

Journal Publication 1 (JP1): *"SatSysSim: A Novel Event-Driven Simulation Framework for DVB/RCS2 Performance Characterization". IEEE ACCESS, 2022*

This paper presents a novel simulation framework capable of providing a detailed assessment of a satellite communication's network performance in realistic scenarios. The proposed framework employs an event-driven methodology, models the communications network as a DES (discrete event system), and focuses on the return link of the DVB-RCS2 standard. Three different scenarios demonstrate possible uses of the simulator's outputs to understand the network's dynamic behavior and achieve optimal system operation. Each scenario explores different features of the simulator covering a large territory with thousands of users, which in our case study was the country of Brazil.

Conference Publication 1 (CP1): *"Game Theory DVB-RCS2 Return Link Fairness Optimization Based on Timeslot Information Payload". SBRT 2021.*

This paper introduces a novel algorithm modification for the conventional game theory-based time slot assignment method applied to the Digital Video Broadcast Return Channel via Satellite (DVB-RCS) system. The procedure considers the spectral efficiency as a weighting parameter for the resulting convex optimization problem of the Nash Bargaining Solution. This approach guarantees the fulfillment of Quality of Service (QoS) constraints while maintaining a higher fairness measure; results show a 5% improvement in fairness, with a 75% decrease in the standard deviation between frames, also managing to reach a 12.5% increase in individual terminal capacity distribution satisfaction.

To the best of our knowledge, there is no similar published study with results obtained by system-level simulations considering an M2M traffic configuration with DVB-RCS2 uplink scheduling for the Brazilian territory. The software implementation contributions of this dissertation consist of the following items:

- Application of the proposed event-driven simulation in large scale DVB-RCS2 deployments.
- Implementation of a flexible platform for the evaluation and comparison of allocation algorithms inside a discrete event simulator.
- Creation of geospacial performance results to extend the analysis of the satellite network running using the proposed framework.

Table 1 – Simulator features

Features	sns3 [31][12]	DVB-S2/ RCS simulator [32][33]	Proposed Framework (SatSysSim)
Easy to maintain	Yes	Yes	Yes
Integration with link level from [34]	No	No	Yes
Join Results with Anatel (Brazilian Government)	No	No	Validation in [35] [36]
Compatible with DVB-RCS2	Yes	Yes	Yes
Control over the source code	Open source	Open source	Proprietary
Extended from	ns-3 [37]	OMNeT++ [38]	Sharc [39]

There are other satellite simulators available in the open literature as well as commercially available software. A comparison of similar computer simulators to the proposed implementation is shown in Table 1. The decision to implement the proposed simulator instead of using existing solutions were based on the following criteria as well as summarized in Table 1:

- **Easy to maintain**: The code base for the proposed implementation is version controlled and extensively tested using standardized approaches to assess simulator behavior.
- **Integration with previous link level platforms [34]**: There exists two other simulator platforms related to the proposed SatSysSim framework. One

is a link level simulator and the other is antenna simulator. The system level simulator were created to provide an easy integration with those other two projects.

- **Join results with Anatel (Brazilian Government)**: The proposed code base framework possesses results employing Anatel contributions related to satellite communications. Sharc [39] possesses several joint contributions with Anatel that have been proposed in ITU meetings [35, 36]. This is important since the primary focus is the Brazil operating environment, and thus needs to consider the scope of the sponsors for this research project.

- **Compatible with DVB-RCS2**: The evaluation scenario for this proposed framework is targeting the Brazilian operating environment.

- **Extension** : This DVB-RCS2 simulator was created extending the functionality of previous simulators.

CHAPTER 2
SATELLITE COMMUNICATIONS

This chapter provides a general and systematic view of the DVB-S2X/DVB-RCS2 standard and its satellite network configuration. We explain the key constraints and goals of satellite communications, elucidating the basis for the scheduler framework and its resource allocation problem, focused on fleet tracking applications. After outlining the system functional view and the standard guidelines, we will explain the design choices for the developed simulator, and in later sections, we explain our proposed solution.

2.1 Introduction

A satellite is a self-contained communication system orbiting Earth. It has the ability to receive and retransmit signals with the use of a transponder [40], i.e., a receiver and transmitter of high-frequency radio signals. When thrown into orbit, a satellite has to withstand the shock of being accelerated to an orbital velocity of 28,100 km/h, which is a structural design challenge, while also withstanding a hostile environment. When in orbit, a satellite is exposed to radiation and extreme temperatures. So it faces several design challenges when put into place and to operate in the vacuum of space.

There is no possibility of maintenance or repair in space. The system is required to be controllable in orbit at all times while maintaining reliable communication back and forth for the entirety of its operational lifespan, which can be up to 20 years. Moreover, as each kilogram added to the equipment raises the cost of the launching mission significantly, it is required for satellites to be lightweight. In this work, we focused on the telecommunication aspect of satellite systems. However, this description clarifies the main differences between satellite communication and the other varieties of telecommunication systems, as the energy-bound constraints frequently appear further in the results.

Satellite communications are governed by the International Telecommunication Union (ITU), a United Nations specialized agency. The International Telecommunications Union (ITU), based in Geneva, Switzerland, receives and approves

applications for satellite orbital slots. The World Radiocommunication Conference is held every two to four years by the ITU, and it is responsible for assigning frequencies to various purposes in different parts of the world. These laws are enforced by each country's telecommunications regulatory agency, which also grants frequency licenses.

2.2 A Brief History of Satellite Communications

Before tackling the problem in its full complexity, we highlight the overall importance of satellite telecommunications. We describe historically how these solutions came to be in the first place, giving context as to why using artificially implemented objects orbiting around the Earth is a viable design choice for network telecommunication systems.

Since the early 19th century, scientists and engineers of the time have already developed enough of the theory of electricity to build the first telegraph, and since then, society has striven to make communications reliable, efficient, and globally accessible. Arguably one of the earliest noticeable landmarks in global communication was the laying of the first transatlantic telegraph cable from Valentia, in western Ireland, to the Bay of Bulls, Trinity Bay, Newfoundland. The first transmission occurred on August 16, 1858, having irreparable design flaws that led to its demise three weeks later.

The successor of the telegraph was the telephone, invented in 1876 and often credited to Graham Bell, who was awarded the first successful patent. However, other inventors such as Elisha Gray and Antonio Meucci also developed similar concepts around the same period. It was not until around 80 years later that an achievement analogous to the first telegraph cable was implemented for telephones: the first transatlantic telephone cable was laid in 1956, connecting the USA to Europe; it was called the TAT-1 (Transatlantic No. 1) cable system, and since then, TAT-2 to TAT-14 were implemented with more reliable and faster technology such as fiber optics. In parallel to the TAT cable systems, which have terminations in the U.S. and usually use the great circle route (the shortest) connecting London to New York, there are three implemented CANTAT cable systems, which terminate in Canada rather than the U.S., and one private transatlantic telephone cable system called PTAT.

The next big step in linking the world together was communication by satellite, using microwaves to operate, i.e., waves with wavelengths λ ranging from around one meter to one millimeter. With high operational frequencies (100 MHz

to 300 GHz), microwaves were first used for communication in the early 1930s. Looking forward 16 years later, in 1946, scientists on the project Diana (named after the moon goddess) used microwaves to bounce electromagnetic signals off the moon and back, an idea that later inspired EME (Earth-Moon-Earth) communications, often used by U.S. Navy engineers at the time to reflect microwave radio communication signals from Washington, D.C. to Hawaii. This experiment was also the first in radar astronomy, allowing the examination of other celestial bodies and to measure their inherent properties.

With the development of modern rockets, many engineers started to ponder the possibility of an orbiting telecommunication element being put into space [41]. It is attributed to Arthur C. Clarke the idea of a geosynchronous communication satellite, which he published in October 1945 in an issue of Wireless World. Clarke believed that a radio relay placed high above the Earth's atmosphere could serve a large area of the Earth's surface, much like a radio tower thousands of miles high. Later, J.R. Pierce of Bell Labs published an article entitled "Orbital Radio Relays", discussing passive satellites and satellites with powered repeaters. He calculated the feasibility of an orbiting satellite with microwave technology, proving it would allow effective communication between two points on Earth.

The idea of an object orbiting around the Earth for communication purposes, a.k.a. artificial satellites, was then considered a possible achievement. The first satellite to contain a radio transmitter was the USSR's Sputnik, launched in 1957. Also, the historical event named "The Space Race" had begun, and both economic superpowers (U.S. and the USSR) were rushing for technological control. Later that same year, the U.S. developed Project SCORE, which launched the first radio relay capable of transmitting and receiving data.

In this first period of satellite communication development, the main applications of satellites were for military purposes. In fact, to this day, military command and control in many countries depends on satellite systems, with some technologies remaining secret due to homeland security reasons. These applications usually involve weather information, voice and data communication, navigational data, spy satellites, and the Global Positioning System (GPS).

The first satellite launched for civilian communication purposes was Echo I, launched in 1960 by NASA and Bell Labs. This satellite consisted of a large plastic balloon, which was inflated in space, with its surface coated with a thin aluminum layer. The idea behind this aluminum layer was to reflect microwave beams aimed at it. Two years later, Echo I was used to reflect microwave signals that consisted mainly of images and telephone conversations. In this same period, other nations,

such as the United Kingdom and Canada, invested in launching satellites.

The objective was then to upgrade the satellite networks with more advanced satellites that contained active electronic relays, to launch a large number of satellites into orbit and to build more ground stations to communicate with these corresponding satellites. In principle, this network could efficiently transmit telephone or television data anywhere at a low cost, and, under this guise, the first satellite to be launched was ATT's Telstar I on July 10, 1962. Telstar I was used for transmissions between the U.S. and Europe, and it was the first satellite to use a traveling wave tube for transmitting microwave signals. Thirteen days after the launch, the first live broadcast of a television show between the United States and Europe took place, showing live footage of New York City and the Golden Bridge.

Satellites like Telstar imprinted a new era, allowing countries across the oceans to be linked through the skies. Although an impressive feat of engineering and telecommunications, non-geosynchronous satellites (i.e., satellites that do not have a fixed point in the sky relative to the Earth's movement) were only visible when orbiting over the horizon line, being available only for a limited amount of time before repeating the cycle. For example, Telstar I was only available for use by the stations in the U.S. and Europe for about 100 minutes per day. It would move across the sky and then disappear over the horizon. So, for any reliable telecommunication system based on non-geosynchronous satellites to take place, a large number of ground stations located all around the world and separated by large distances would be necessary. This network would need connections through each other via legacy wired links or, alternatively, a large constellation of satellites.

The solution to this problem was to implement the geosynchronous satellite envisioned by Arthur C. Clarke back in time. A geosynchronous satellite has an orbital speed that matches the speed of the Earth's rotation, making it appear as a fixed point in the sky. This meant that the satellite would be available constantly, never dipping below the horizon. In 1965, the satellite named Early Bird I was launched; it was the first satellite with a geosynchronous orbit and could provide 150 simultaneous telephone links or one television link. In fact, this orbit design largely simplified the problem of space-to-ground communication and, until today, is one of the most commonly used orbit schemes for telecommunication satellites.

It was in 1969 that global satellite coverage was achieved, just a few days before the first moon landing, and, as a consequence of this, it was possible to broadcast this event worldwide on live television. Later on, other applications for satellites sprouted back in the 70s, such as navigational aid for commercial ships. Suddenly, domestic satellites appeared to enhance or bypass existing land-based na-

tional networks, not aiming to provide international links across the oceans. Canada was the first nation to adopt domestic satellites, it has a large body of land with vast rural areas that were poorly covered by the existing telephone system. It was then common for many other countries to purchase or lease satellites to avoid the high expense of building ground-based telephone, radio, or television networks.

In the late 1970s and 1980s, new domestic satellite networks emerged, using satellites to create a low-cost alternative to the more expensive land-based broadcast service provided by earlier television broadcasting companies in the U.S., such as NBC, ABC, and CBS. In these systems, ground stations operated by the local cable companies receive the signals and retransmit them over coaxial cable to the consumer's home. Since then, technology has evolved and the satellite television broadcast signal is transmitted directly to a receiving dish antenna mounted outside of the consumer's house, pointing directly towards the satellite transmitting the television broadcast. The Earth-to-satellite link was possible due to high-power transmitters, more sensitive receivers, and higher frequencies that allowed for smaller components and antennas.

2.3 Satellite applications

Satellite technology has progressed from the experimental (Sputnik in 1957) to more sophisticated and powerful satellites in a relatively short period of time. Constellations comprising tens of thousands of satellites are being developed to provide global Internet access. Future communication satellites probably will have more onboard computing power, larger aperture antennas, and larger onboard processing capabilities, allowing them to manage more bandwidth. Satellite propulsion and power systems will be improved further, increasing their service life to 20–30 years from the existing 10–15 years.

Each year the demand for video, voice, and data traffic increases, requiring more bandwidth to support the communication networks. The development of new telecommunication applications continuously fuels the demand for satellite services. The desire for increased bandwidth, continued innovation and development of satellite technologies defines a commercial incentive for the satellite industry's long-term survival well into the twenty-first century.

As explained in Oltjon Kodheli et al.[42], satellite communication have been used for a variety of purposes since their debut, including media broadcasting, earth observation, backhauling, and newsgathering. Nevertheless, there is a new wave of applications being developed, and the paradigm of satellite communications is cur-

rently passing through a transformation phase, focusing the system design on data services as a result of the rise of Internet-based applications, namely broadband systems. Oltjon Kodheli et al. [42] indicate the two main motivations for this change: firstly, the rapid adoption of media streaming instead of the typical linear media broadcasting systems, and the second reason can be attributed to the necessity to extend broadband coverage to under-served areas, such as developing countries, aerospace/maritime and rural areas. Figure 1 illustrates possible applications of satellites in this new context of 5G communication.

Furthermore, the integration and convergence of various wired and wireless technologies is a major milestone in the 5th generation of communication systems (5G). Satellite communications, in this context, pave the path for an integration aimed at specific use cases that may just benefit from their distinctive features. And in parallel to this, private businesses have created a variety of production and launch choices that were previously only available to governments and a few large international corporations.

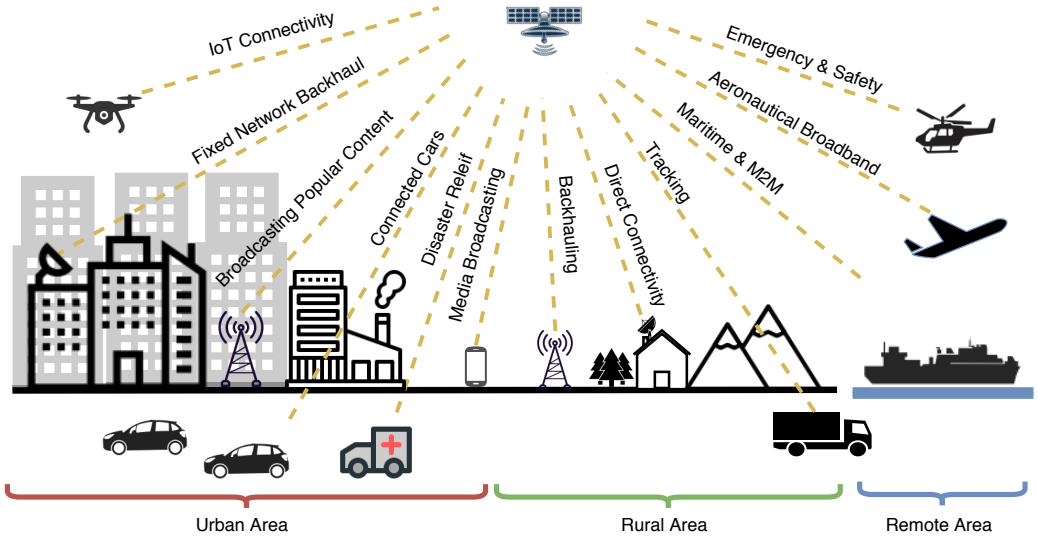

Figure 1 – Diagram describing the role of satellite communications in the 5G communication ecosystem, adapted from [42].

Now that we are contextualized, we can dive into the technical details. Firstly, we will take a top-down approach, specifying the systems from a bird's eye point-of-view, over-viewing the general environment. Then we will work upon and progressively taper into the specific implementation choices to justify every step of the way.

2.4 Satellite Communication Systems

We will further detail some other aspects relevant to the total description of a satellite system, summarizing the possible orbits, the telecommunication capabilities of current satellite systems, the usual operation frequency ranges, and some important constraints parameters. We also explain the motivation for the choice of the DVB-RCS2 standard before tackling the complete description of its subsystems.

The essential components of a satellite can be grouped into three main systems: the communications system, which includes the antennas and transponders that receive and rebroadcast signals; the power system, which includes the solar panels that generate power; and the propulsion system, which includes the rockets that drive the satellite.

A satellite requires its own propulsion system to arrive to the proper orbital location and to make periodic modifications to that position. The gravitational forces of the Moon and Sun can cause a satellite in geostationary orbit to wander from its original location. As a result, thrusters are fired on a regular basis to change its position. An earth station is responsible for maintaining this task. The amount of fuel used to power these thrusters determines the lifespan of a satellite, and when the satellite's fuel runs out, it wanders into space and ceases to function.

A satellite in orbit must operate constantly and be controllable for the duration of its life. It requires internal power to run its electronic systems payload. The major source of electricity is solar power, which is captured by the solar panels on the spacecraft. A satellite also has batteries onboard to provide electricity when the Earth blocks the sun and to store extra energy from the current created by the solar panels.

A satellite link has a tracking, telemetry, and control (TTC) system. It is a two-way communication link between the satellite and the Network Control Center (NCC) on the ground that enables a ground station to track the position of the satellite and operate its propulsion, thermal, and other systems. It can also monitor the satellite's temperature, voltages, and additional critical factors.

The gradual evolution of telecommunications technology, such as the use of digital systems and the miniaturization of electronic components, allowed for a boost in satellite capacity throughout the years. For example, the Early Bird satellite previously mentioned had only one transponder and it could only broadcast one T.V. channel; now, we can have satellites providing over 1,600 TV channels, with each transponder allowing multiple channels.

2.4.1 Satellite Orbits

Satellites operate in a few different orbits, the most usual being:

- **Low Earth Orbit (LEO):** The satellites are positioned at an altitude between 160 km and 1,600 km (100 and 1,000 miles). In LEO orbits, as the satellite orbits closer to the Earth's surface, the link quality tends to be greater than its higher-orbit counterparts. LEO orbits require 20 or more satellites for global coverage.
- **Medium Earth Orbit (MEO):** In this orbit the satellites operate from 10,000 to 20,000 km (6,300 to 12,500 miles) from Earth. MEO orbits require 10 or more satellites for global coverage.
- **Geostationary orbit (GEO):** The satellites are positioned 35,786 km (22,236 miles) above Earth, they complete one orbit in 24 hours and thus remain fixed over one spot. It takes only 3 GEO satellites to provide global coverage, in contrast to LEO and MEO orbits.
- **Polar Orbit.** This orbit passes roughly through the Earth's poles, moving longitudinally as it orbits around Earth, instead of having a west-to-east movement common in the other orbits. This class of orbit is very common for earth observation satellite systems.

There is a range between LEO and MEO orbits (called the Van Allen radiation belt) that satellites cannot operate, as the electronic components are affected by solar explosions and radiation steered by Earth's magnetic field. Different from GEO orbit, communicating with satellites in LEO and MEO requires tracking antennas on the ground to ensure a seamless connection between satellites.

2.4.2 Frequency Bands

Satellite communications use very high-frequency ranges to broadcast and receive signals, ranging from 1 to 50 GHz. A subset of this range uses letters as labels such as L, S, C, X, Ku, Ka, and V bands (shown in table 2), ordered from low to high frequency. Signals in the lower end of the satellite frequency spectrum, such as L, S, and C bands, are sent with less path attenuation, with the trade-off that larger antennas are necessary to receive them. Signals in the higher end of the spectrum, such as X, Ku, Ka, and V bands, allows the use of smaller reception antennas, in fact, they can be received by dishes as small as 45 cm in diameter, and

as a result, the Ku and Ka-band spectra are ideal for DTH broadcasting, broadband data transmission, and mobile telephony.

Table 2 – Table for the nomenclature and range of radio-communication bands (adapted from ITU [43]).

Letter symbols	Radar (GHz)		Space radiocommunications	
	Spectrum regions	Examples	Nominal designations	Examples (GHz)
L	1-2	1.215-1.4	1.5 GHz band	1.525-1.710
S	2-4	2.3-2.5 2.7-3.4	2.5 GHz band	2.5-2.690
C	4-8	5.25-5.85	4/6 GHz band	3.4-4.2 4.5-4.8 5.85-7.075
X	8-12	8.5-10.5	–	–
Ku	12-18	13.4-14.0 15.3-17.3	11/14 GHz band 12/14 GHz band	10.7-13.25 14.0-14.5
K	18-27	24.05-24.25	20 GHz band	17.7-20.2
Ka	27-40	33.4-36.0	30 GHz band	27.5-30.0
V	–	–	40 GHz band	37.5-42.5 47.2-50.2

One detail to touch upon before introducing further topics is that the communication link quality (and consequently the data rate) is affected by the weather conditions. The DVB standard dynamically changes the coding rate of error correction codes and the order of the digital modulation to restrain this effect and maintain the system capacity. The rain is the meteorological event most relevant for the link quality decline. It can have a duration of many minutes, so the variation in the modulation and code rate has about this order of magnitude. Figure 2 presents qualitatively this characteristic evolution of the rate transmitted and the rain conditions.

As detailed by J.B. Dupé [21], there are two processes that have a major impact on the scheduling and resource allocation for satellite telecommunication systems: firstly, the dependence that link quality has on meteorological changes, specifically that high-frequency signals have a larger sensibility to water vapor attenuation, and secondly that resource allocation depends on the system utilization, i.e., it depends on the number of active terminals and on the capacity of the system to forward a sufficient amount of resources to these terminals (in our case, called RCSTs).

There are notable differences between satellite and mobile links. Satellite links present little to no multi-path attenuation but are highly affected by mete-

orological phenomena, because they have longer link lengths to connect with the orbiting satellite. The variance of the signal quality with geographical location can dramatically change the allocation fairness in most scheduling algorithms. This observation leads to the proposed game theory-based scheduling algorithm for this work.

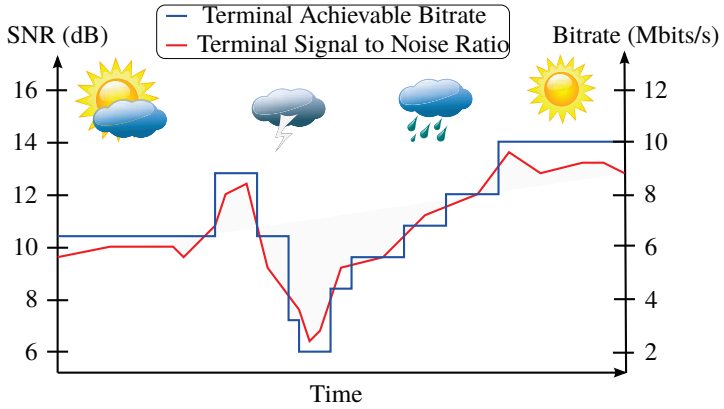

Figure 2 – Relationship between the weather conditions and the maximum bitrate capacity achievable, adapted from [21]

For precise numerical values for the attenuation by water vapour, gases, air, etc, we can refer back to the ITU standard [44], for example Figure 3, which shows the increasing relationship between the attenuation and the link frequency for the link's zenith, and because satellites work at very high frequencies, the attenuation is relevant for the total bitrate achievable.

The relationship between the link SNIR and the environment had a static treatment in the first generation of the DVB standard, which meant that the system accuracy was highly dependent on the availability of meteorological data and rough interpolations of the link quality. The static nature of the link control was not necessarily a problem in the first generation standard, as the intended application was Television/Video broadcasting, which used a frame Moving Picture Expert Group (Mpeg-2) with a fixed length of 188 bytes, meaning the necessary rate could be calculated based on the Video Codec used. Although historically the DVB standard was expected to handle only television broadcast applications, it expanded further in scope for IP encapsulation applications.

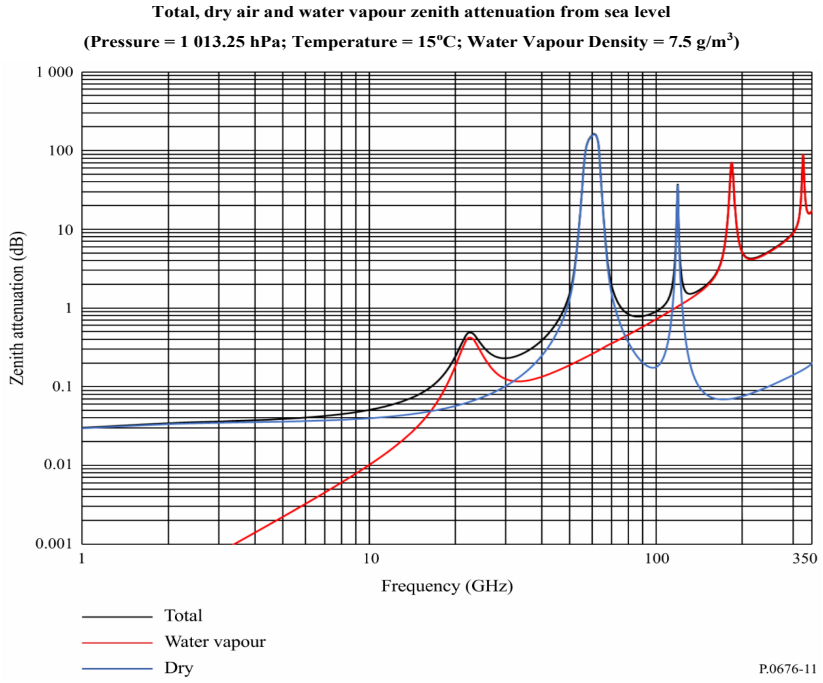

Figure 3 – Relationship between the link's frequency and the Zenith attenuation by water vapour and dry air, adapted from [44, p. 29]

2.5 The DVB-S2X/DVB-RCS2 Standard

The first DVB implementation was characterized by a worst-case scenario statistical dimensioning, not expecting the dynamic variables that might affect the scheduling. This particularity was changed in later standards (DVB-S2/DVB-S2X) as the possibility of control data transmission/reception allowed for new applications to emerge, among them the fleet tracking application. Telecommunications for fleet tracking is characterized by a high number of simultaneous users, there is a high variance for the terminals geographic position and there is a dynamic demand for data rates. This implementation would be possibly unattainable or very restricted with the first generation technology.

DVB-S is the most accepted and widely spread standard in the satellite market [45]. The standard has a deep market penetration in sports and news contribution, professional video distribution solutions, IP trunking, cellular backhauling, and broadband VSAT solutions. As new technologies (HTS, HEVC, UHDTV) emerge, data rates increase at an accelerated pace. The DVB-S standard has the following features:

DVB-S (Digital Video Broadcasting - Satellite):

- Published by ETSI (EN 300 421) in 1994 and evolved in 1997.
- Modulation scheme: Single Carrier QPSK.
- Coding: Reed-Solomon (Outer) + Convolutional (Inner).
- Rolloff $\alpha = 0.35$.
- Input Stream: Single MPEG transport stream for standard TV.

The demand for higher speeds, more efficient satellite communication technology, and wider transponders required DVB to support the exchange of large and increasing volumes of data, video, and voice services over satellite. In 2005 the DVB-S2 standard was introduced, with features that allow Bandwidth on Demand (BoD) and Demand Assigned Multiple Access (DAMA) scheduling policies. These features were made possible with the introduction of different techniques, such as variable frame lengths, pilots in the control header, dynamic estimation of the link quality, and finally, adaptive alternatives for modulation, coding rates, and roll-off factor. Some of the the main highlighting features are:

DVB-S2 (Digital Broadcasting - Satellite Second Generation):

- Ratified by ETSI (EN302 307-1) in March 2005.
- Designed for HDTV and internet access, support H.264 (MPEG-4 AVC) codec.
- Variable coding and modulation (ACM) to optimize bandwidth.
- Added 8PSK, 8/16/32 APSK higher order modulation schemes.
- Added rolloff = 0.20 and 0.25
- Coding: LPDC + BCH (Outer).
- Frame: Header + Data.
- Support both IP packet data and MPEG-TS stream.

With the development of more applications that test the limits of the DVB-S2 standard and its efficiency requirements, an improvement to the DVB-S2 standard called DVB-S2X was released. The new DVB-S2X features a combination of reduced roll-offs (5%, 10%, and 15%) and enhanced filtering technologies to allow for optimal carrier spacing. When compared to DVB-S2, the combination improves efficiency by up to 15%. The DVB-S2X standard expands the number of MODCOD schemes and

Forward Error Correction (FEC) options. Adding higher modulation schemes such as 256APSK proved to be useful in professional applications with improved link budgets provided by larger antennas. The DVB-S2X extends the following features:

DVB-S2X (DVB-S2 extension):

- Standardized by ETSI (EN302 307-2) in March 2014.
- Added 64, 128 and 256-APSK modulation schemes.
- Finer MODCOD (modulation and code rate with 116 combinations).
- Added rolloff $= 0.05, 0.10$ and 0.15.
- Data scrambled at baseband.
- Channel bonding up to 3 channels.
- Support UHDTV quality.
- Very low SNR operation.
- Enable satellite network to effectively support LEO and MEO (low and Medium Earth Orbits).

DVB has added nine additional MODCODs to the DVB-S2X standard throughout the QPSK and BPSK ranges. This allows satellite networks to withstand significant atmospheric fading and use smaller antennas for on-the-go applications (land, sea, air). These Very Low Signal-to-Noise Ratio (VL-SNR) MODCODs improve the satellite link's robustness and availability, and unlike DVB-S2, which has only linear MODCOD schemes, DVB-S2X MODCODs are divided into two classes: linear and non-linear MODCODs.

Now that we introduced the overview of the DVB standard and its features, we can dwell on the specific aspects of resource scheduling and capacity requests for DVB systems.

2.5.1 DVB Standard Return Link Architecture

From a functional perspective, satellite telecommunication systems resemble terrestrial wireless networks, but there are differences from their terrestrial counterparts. The term "Satellite Telecommunications" is an umbrella term that encapsulates, among others, the networks for data gathering (e.g., Argos), navigation (GPS, Galileo), or even the networks reserved for telephony (Inmarsat, Iridium).

Brazil has a continental scale and an extensive collection of fleets. This as-

pect becomes relevant for the design choices of the simulator implemented, as the development relies on simulating realistic fleet tracking scenarios. In fleet tracking applications, the telecommunication terminal is installed directly on the moving truck, implying that the radio needs to track and communicate with the GEO satellite properly as the truck moves around the country.

The DVB standard implementation guidelines [7] defines a reference model for mobile scenarios and, more generally, the nomenclature for elements in this category of networks.

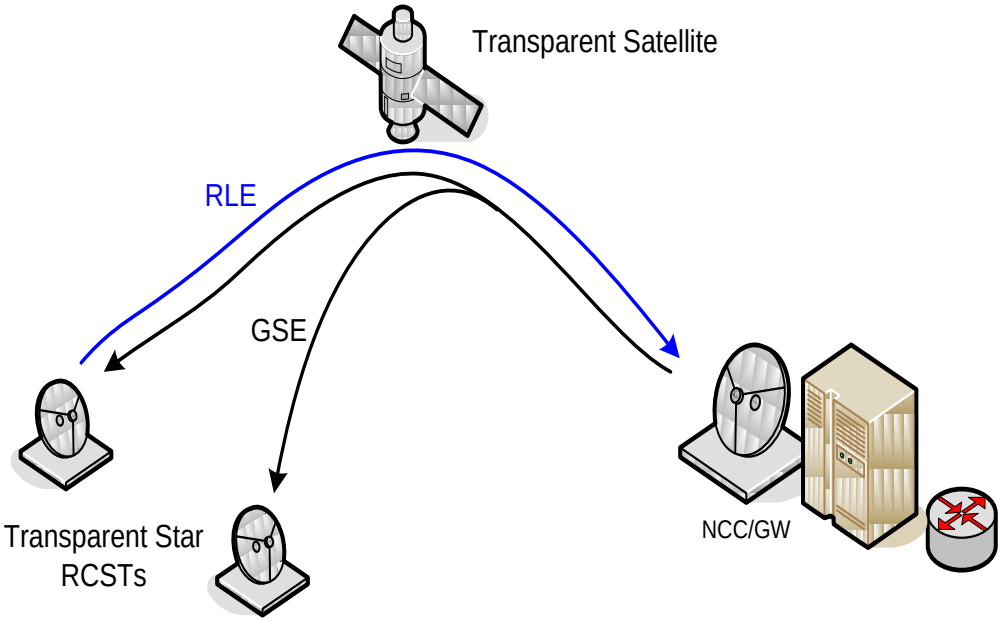

Figure 4 – Star-only topology scenario for communication in DVB systems for Transparent Satellites (adapted from [7]). RLE stands for Return Link Encapsulation and GSE stands for Generic Stream Encapsulation.

The communication is based on a broadcast network with a star topology between the Network Control Center (NCC) and the mobile terminals (RCSTs). The GEO satellite works as an intermediary between these broadcast links. The forward link conforms to the Digital Video Broadcast for Satellite Communication standard (DVB-S); the DVB-S2X is its latest iteration, and the return link is based on the Digital Video Broadcast Return Channel standard (DVB-RC), where DVB-RC2 is its latest version. Figure 4 describes the network topology of these star-only connections with transparent networks.

The forward communication (from NCC to the terminals) is based on Time Division Multiplex Access (TDMA), while the return link (from the terminals to

NCC) is based on Multiple Frequency Division Time Division Multiplex Access (MF-TDMA). We study the resource management of the scheduler in the DVB-RCS2 link, as this broadcasting paradigm has a large number of terminals that share the same channel capacity resources. This implies the demand for an optimized scheduling strategy to avoid poor queueing management problems (e.g., starvation), a problem that affects the overall quality of the connection and the service experience.

As they are frequent throughout this text, we describe these three acronyms:

- **Network Control Center (NCC):** This is the HUB where all the incoming traffic is controlled. Here, the control center receives the traffic from all the mobile terminals and makes scheduling and capacity allocation decisions. The NCC is responsible for planning all the communication, with a series of planning tables transmitted to each terminal that define the scheduled time and frequency that a given terminal will transmit in the MF-TDMA frame.

- **Return Channel Satellite Terminal (RCST):** The RCST is the mobile terminal. In our context of fleet tracking, the radio is placed on the fleet and tracks the GEO satellite. To communicate properly with NCC, it requests capacity from the NCC based on its internal processes demands.

- **Satellite operator (SO):** The SO controls the satellite outside the scope of the network planning, guaranteeing the functional operation of the satellite. The satellite company provides this service.

The NCC communicates with multiple RCSTs through a satellite. In the forward link, the NCC periodically sends messages to the RCSTs, such as the MF-TDMA structure and the MODCOD schemes, based on the RCSTs channel conditions. The RCSTs respond with packet bursts in their allowed time and frequency slots within the MF-TDMA structure. The DVB-RCS2 standard allows Adaptive Code and Modulation (ACM) and Dynamic Rate Adaption (DRA) [46, 47] channels to improve spectral efficiency. RCST's transmission parameters, such as code rate, modulation order, and symbol rate, are based on NCC's estimates of signal to noise plus interference ratio (SNIR). It is a bandwidth-on-demand solution where the NCC must calculate the number of resources to assign to each corresponding terminal, characterized by Demand Assigned Multiple Access (DAMA). RCS2 allows four different types of assignments:

- **Constant Rate Assignment (CRA):** Requires a constant rate based on the Service Level Agreement (SLA) between the RCST and the service provider.

- **Rate Based Dynamic Capacity (RBDC):** The RCST requests a certain bit rate constraint to be met that remains effective until updated.

- **Volume-Based Dynamic Capacity (VBDC):** The RCST uses this capacity request when it knows the amount of data to transmit, making a request based on the volume of data and not on data rate.

- **Free Capacity Assignment (FCA):** In this modality, without an RCST request, the NCC assigns the surplus of capacity not allocated in the current scheduling iteration.

The DVB-RCS2 [48] makes use of a hierarchical and flexible frame structure. The minimum resource block that composes the frame is named bandwidth-time unit (BTU), which has a configurable length (in symbols) and symbol rate.

A Timeslot (TS) is a contiguous sequence of BTUs in time. A TS may possess a different size based on the number of BTUs assigned to it. Furthermore, a TS is the minimum allocation unit used by the packet scheduler. Users with different throughput requirements may be allocated to TSs of different lengths, which allows the allocation algorithm to manage radio resources. All lengths allowed by the RCS2 physical layer standard [6], which are also called burst lengths, are defined by the amount of data symbols assigned to a set of distinct Adaptive Modulation and Coding Schemes (ACMs).

Here, we consider allocating the SuperFrame (SF) structure inside the MF-TDMA hierarchy, where the BTU (bandwidth-time unit) is the minimum allocation unit in the time-frequency grid. An RCST is assigned to a TS, composed of one or more BTUs. Different MODCODs require TSs of different sizes due to their different payloads.

RBDC and the VBDC are the only types of requests in which there is a possibility of defining a scheduling strategy that optimally assigns users in an SF optimal manner, that in this context means that (i) the allocation is fair in the sense of the Jain fairness index; (ii) the QoS requirements are met, and (iii) the BTU resources are not being wasted. We look for optimal allocation algorithms, having both a fair distribution to each RCST and a feasible data-rate efficiency while maintaining low operational complexity. Computational speed is relevant because the NCC must broadcast the complete specification of RSCT's TSs through the Terminal Burst Time Plan Table (TBTP) at every SF. Typical SF duration is between 100 ms and 1 s, e.g., 256 ms [24].

Although we largely focus on the DVB-RCS2 (i.e., the return link) scheduler, any technique applied here can be used for the forward link as a simplified case.

Figure 5 shows a summary of the division elements in the SF structure, where we see the hierarchical elements of the SF, as the frame, which is a set of TSs arranged in both time and frequency. It is incorporated into a SF, an arrangement of frames ordered both in time and frequency. A superframe sequence (SFS) is an ordered time sequence of superframes. An RCS2 system may use different SFSs within a satellite transponder according to the overall bandwidth requirements or capacity restrictions. From an allocation algorithm perspective, a user is a TS number identified by its position inside a particular frame within an SF. The global configuration is communicated to all RCSTs by tables (SCT/FCT2/BCT/TBTP2) that are broadcast to all users via a signaling procedure. Details can be found in ETSI EN 301 545-2. [6] and ETSI EN 301 545-4 [7].

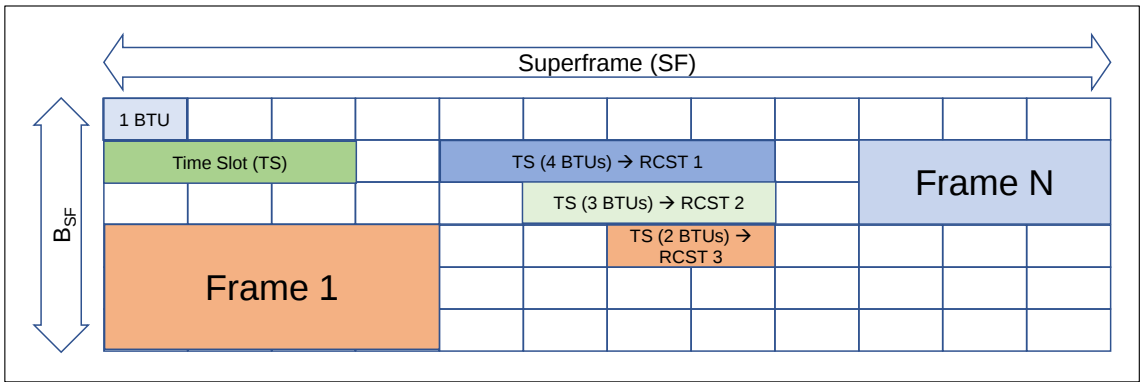

Figure 5 – Diagram illustrating the hierarchy of elements in the DVB-RCS2 SF.

Now that we have explained the DVB standard resource allocation scheme, the next step is to discuss the allocation problems that this structure implies. The following chapter is dedicated to a summary of three subjects: queueing theory, the resource allocation problem, and discrete event simulation. These topics are necessary to describe our algorithm for the DVB MF-TDMA scheduler.

CHAPTER 3

THEORY OVERVIEW

3.1 The Game Theory Framework

Game theory is a branch of mathematics that defines a framework for modeling systems of interactions among rational decision-makers. Using this general field, one can categorize and define solutions for many problems, based on certain predefined solution criteria that depend on the nature of the game played. Game theory is a broad body of study in applied mathematics, being used to solve problems in many research areas such as economics, control theory, computer science, psychology, biology, and sociology.

Game theory was initiated by the famous mathematician John Von Neumann and Oskar Morgenstern [49], later being expanded by other important contributors such as John Nash, who, among his contributions, introduced an axiomatic solution to the bargaining problem. He added five axioms that determine a solution in the space of outcomes for cooperative games. Later, this solution was modified by Ehud Kalai and Meir Smorodinsky. Nash also played an important role in proving the existence of a mixed strategy equilibrium in every finite game using the Kakutani fixed-point theorem (or the Brower fixed point theorem in its original thesis). This latter topic will be out of scope, but is important to comment for historical context purposes.

Game theory is the study of decision making under competition, and in a plethora of problems studied by game theorists, the main goal is to define the optimal decision making strategy, given that an individual (or player) decision affects the outcome (and payoff) of a game for all the other individuals. The whole field is commonly divided into four main subcategories of study [50]:

- **Classical Game theory:** Focused on finding the optimal play in situations where multiple players are involved, in which they are part of the decision making process, and where the impact of those decisions (also called strategies) on the final outcome is known for each individual involved.

- **Combinatorial Game theory:** This subcategory focuses on games with two players, such that each player takes turns in predefined ways. In this category, games like chess, go, and etc. are studied. "Combinatorial' game theory has this name because such games scale in complexity in non-polynomial time, making it necessary to rely on combinatorial theory to explore the possible solutions and outcomes.

- **Dynamic game theory**: This branch studies the dynamics of a game over time, and it takes into consideration the order of decision making in time. Decisions will affect the outcome differently at each moment in time, so it relies on differential equations to model the net behavior in the game at each time step. One important application of this concept is the study of traffic behavior. By interpreting each car as a player trying to optimize its outcome, we can predict its decision making process in different road scenarios. That way, it is possible to predict and apply these solutions in real urban design.

- **Other topics in game theory:** Game theory is a broad concept, and here we have an umbrella category to group all the other extended branches covered by this term. Examples include evolutionary game theory and experimental game theory; the former is important for studying evolution and species competition in biology, while the latter is used to determine how well classical game-theoretical models explain real-world behavioral scenarios.

There are three main approaches to represent a game in the game theory framework, these are:

- **Extensive form game:** Represents the game with all of its sequential moves and sub-games, with the help of graph theory, assigning to each vertex a player and to each terminal vertex a final payoff. This is a more general representation of a game and can define unique equilibrium solutions that might be missed by the other two forms. As in our scope we are dealing with simultaneous move games, such as the bargaining problem in its basic form, we will not delve into this subject.

- **Normal form game:** It represents the game based on its final payoff function, then tries to find the solution or the equilibrium for the game based on the set of possible outcomes. By understanding some basic properties of those spaces and defining the meaning of solution axiomatically, it is possible to choose the best strategies to maximize utility. We chose to analyze this type of game thoroughly in this work, as it is the common formulation for the bargaining

problem. The bargaining solution is defined over a convex payoff space mapped from the individual strategies tensor, concepts that will be formally defined in the next paragraph.

- **Strategic form game:** This category of game representation is used commonly for two or more players constant sum games, it is focused on the linear properties of the payoff matrices for each individual playing, usually being compressed in few matrices than the original space as the constant sum properties define linear equations. In fact, in the two-player case the system can be represented as a quadratic form with the canonical basis, which is well know to be a convex function, then it is possible to use the convex optimization tools to solve the resulting problem. One famous result from games in strategic form is the min-max equilibrium solution for zero-sum games.

Definition 1 ***Normal Form Game [51][p.4]:*** *A game G in normal or strategic form is a triplet $G = (I, (S_i)_{i\in I}, (\phi_i)_{i\in I})$, where:*

1. I is a set of players $I = \{1, 2, 3, \dots N\}$
2. S_i is the set of feasible strategies for each player i. we call $S = \prod_{i\in I} S_i$ (i.e. the set of the Cartesian product of the strategies) the strategy profile.
3. ϕ_i is the payoff (or utility) function $\phi_i : S \to \mathbb{R}$ for the ith player.

Games are classified in various ways, usually based on the nature of their payoff space $P = \prod_{i\in I} \phi_i$ (i.e the Cartesian product of all possible payoffs). The most common classifications are:

- **Cooperative / Non-cooperative:** A cooperative game is a game where the players can make coalitions to guarantee the best possible outcome; they can cooperate in order to optimize their final payoff. As the scheduler in the DVB-RCS2 allocation scheme is the central policy maker, it can define an optimal allocation strategy accounting for all the RCSTs requests, so it acts as the coalition in this resource allocation context.
- **Symmetric / Asymmetric:** In symmetric game the payoff space P is symmetric, meaning that the payoff depends only on the strategies employed, not on who's playing them. The resource allocation bargaining game is normally symmetric, unless a priority is defined for each player.

- **Zero-sum / Non-zero-sum:** Zero-sum games are those in which the player's choice cannot alter the amount of available resources, meaning that the gain of utility from one player becomes the loss of another in the same proportion. If we define the utility of players in a resource allocation system based on the amount of resource available, this game can be zero-sum or non-zero-sum, depending on how this utility function is defined.

- **Simultaneous / Sequential:** In simultaneous games each player make its move simultaneously, while in sequential games one player has to make its strategy based on previous moves made by other players. In the DVB-RCS2 scheme, the resource allocation is defined per SF, so the scheduling game is simultaneous in this sense.

- **Perfect/ Imperfect information:** A perfect information game is one where all players have the moves made by other players available, as well as their utility functions and their payoffs, at all times in the game.

In the context of DVB-RCS2 resource allocation for the MF-TDMA frame, we can consider the RCSTs to be the players, each with a utility function associated with the number of timeslots allocated. The DVB scheduler's job is thus to maximize overall utility at each allocation span.

We can think of this system as a cooperative, perfect information, simultaneous game, in which every RCST wants to maximize its individual utility. In fact, this context of resource managing/sharing with limited capacity allows the use of the Nash Bargaining solution, as each player competes for a share of a symbolic cake in a (usually) zero-sum scenario.

3.1.1 The Bargaining Problem

When developing a policy for allocating timeslots in the MF-TDMA frame, we engage in a cooperative game in which every RCST has a vested interest: to receive resources as close as possible to their capacity request, while this preference conflicts with the interests of the other RCSTs, especially when the requests overload the total capacity the system can provide. Although this dilemma appears to be a highly non-cooperative game at first glance, given that each player gains no utility from assisting the others in achieving their goals, there are incentives for players to cooperate with each other: the existence of strategies that, on average, are more likely to benefit the group.

Observing this system, the following questions arise: What is the most natural way of defining an allocation policy for games when there are conflicts of interest? How can they be modeled? Is there any feasible solution that conforms to practical application constraints? Bargaining theory, which is a sub-field of game theory, offers a very concise and elegant way of modeling policy formation problems. In fact, it is used often in the academic literature for resource allocation and other telecommunications scenarios (e.g. [52, 53, 54], among others). .

The famous mathematician John Forbes Nash, in 1950, proposed the first solution to the bargaining problem for two person cooperative games [55]. This solution was readily generalized for the N-th player's case. In fact, among the various approaches to the solution of the bargaining problem at the time, the Nash solution was particularly compelling as it provides an internally consistent framework which is based on strong theoretical foundations (axiomatic constraints). The Nash Bargaining Solution provides a well-behaved solution with desirable properties. In another note, as it is common in the game theory branch of knowledge, this solution broadened itself to influence many important philosophical and economic movements, such as John Harsanyi's (who also explored the bargaining problem) model of social power [56].

When proposing an analytical framework for determining policy solutions for multiplayer games, one must specify the nature of the interactions between the policymakers and their special interests. The approach that Nash employs with his solution abstracts these details, identifying the outcome with the conditions that naturally would be satisfied by a game with rational players. These conditions are called axioms, from which a set-theoretical analysis can be derived.

Here we describe the model of bargaining used throughout this work [57, p. 30]: the N-th person cooperative bargaining problem with fixed disagreement payoffs. We consider the game in its normal form with N players. The payoff vector $\boldsymbol{\phi} = (\phi_1, \phi_2..., \phi_N)$ is an element of a subspace $P \subset R^N$ called the payoff space, which is assumed to be compact and convex. Compactness implies that P is a closed and bounded set, which implies the existence of a minimum for any convex function defined on P, whereas convexity ensures this minimum to be unique. In the payoff space P, there is a special point $\mathbf{t} = (t_1, ..., t_N)$ called the disagreement payoff vector, which is defined as the vector with elements t_i, which is the payoff received by the player i if all players fail to agree.

Let $P^* = \{\phi \in P : \phi_i \geq t_i \forall i \in I\}$, this is the subset of P with all payoffs greater than (or equal) the disagreement payoff. Given a solution to the bargaining problem $\overline{\boldsymbol{\phi}} = (\overline{\phi}_1, \overline{\phi}_2, ..., \overline{\phi}_N)$, we try to interpret what features this solution must

have if all players are individuals acting rationally.

The Nash Bargaining Solution (NB) defines 5 axioms to determine what a solution to the bargaining problem means. These axioms are:

- **Individual Rationality (IR):** No player would agree to receive less than what would be assigned to him if all players disagreed. That is

$$\overline{\phi}_i \geq t_i, \quad \forall i \in I; \tag{3.1}$$

  That condition is necessary so that the solution $\overline{\boldsymbol{\phi}} \in P^*$.

- **Pareto Optimality (PO):** No player would accept a solution where it could make itself better without making any other player worse. This condition alone defines a set of possible solutions H^*, called the "negotiation set". This set does not define a unique solution, which require other three axioms: one defining a constraint given symmetry in the payoff space P^* and another two determining the behavior of the solution under transformation of the payoff space.

- **Symmetry (SYM):** In this context, the space P^* is said to be symmetric if given any point $(a_1, a_2, ..., a_N) \in P^*$ and any permutation of indexes $\sigma : I \to I$ then the point $(a_{\sigma(2)}, a_{\sigma(2)}, ..., a_{\sigma(N)}) \in P^*$. The symmetry axiom of the bargaining solution defines that if P^* is symmetric, then the bargaining solution is $\overline{\phi}_1 = \overline{\phi}_2 = ... = \overline{\phi}_N$. This is defined to guarantee that the bargaining problem does not discriminate between players, only their payoff functions.

- **Affine Transformation Invariance (AFFINV):** Given a payoff space P^*, if a second game is defined as $P_2^* = \mathbf{A}P^* + \mathbf{b}$, where $\mathbf{A} \in \mathbb{R}^n \times \mathbb{R}^n$ is a linear transformation matrix and $\mathbf{b} \in \mathbb{R}^n$ is a vector. The payoff space of the second game is an affine transformation of the payoff space of the first game. Let $\overline{\mathbf{v}}$ be the bargaining solution of this problem, then by the Affine Transformation Invariance axiom $\overline{\mathbf{v}} = \mathbf{A}\overline{\phi} + \mathbf{b}$.

- **Independence of irrelevant alternatives (IIA):** Let G be a game with payoff space P^*, if G^* is a restriction of the game G, i.e., if Q^* is the payoff space of G^* such that $Q^* \subset P^*$ and $(t_1, t_2, ..., t_N) \in Q^*$, $\overline{\boldsymbol{\phi}} \in Q^*$, then this axiom defines that $\overline{\boldsymbol{\phi}}$ is also the solution of game G^*. This means that any sub-game defined in a subspace of the payoff space of a given game that includes the solution of this game, has as a solution the solution of the ambient space game.

Given these five axioms: IR, PO, SYM, AFFINV and IIE, Nash demonstrated that there is a unique solution $\overline{\boldsymbol{\phi}}$ to the bargaining problem given a fixed disagreement point, that is

Definition 2 ***(Nash Bargaining Solution):*** *Let G be a bargaining problem with a fixed disagreement point $\mathbf{t}$, the unique solution that satisfy simultaneously the axioms IR, PO, SYM, AFFINV and IIE is*

$$\overline{\boldsymbol{\phi}} = \max_{\boldsymbol{\phi}} \prod_{i=0}^{N-1} (\phi_i - t_i) \tag{3.2}$$

$$\text{s.t. } \phi_i \geq t_i, \quad \forall i, \tag{3.3}$$

$$\boldsymbol{\phi} \in P^*, \quad \forall i. \tag{3.4}$$

Notice that this solution is in optimization format. The Nash bargaining solution is the arguments that optimize this predefined objective function, and although the NB objective function is not convex, we can workaround this limitation and use convex optimization tools to solve this problem numerically in an effective way. This is explained in detail in the implementation chapter.

It is undeniable that an axiomatic approach brought a shift to the cooperative game paradigm, giving a quantifiable metric and underlying the benefits of standardizing the management of conflicts in a limited resource setting. However, as with any model, there are some limitations, both to the Nash bargaining solution and to the axiomatic framework as a whole. These limitations give rise to different axiomatic solutions that prioritize other trade-off properties. When used to describe more nuanced systems, the bargaining solution might need a more robust set of policies in order to avoid designing a collective structure that converges to a catastrophic solution, which is usually met in economic or political systems, as described in Harsanyi's book.

After the Nash Bargaining solution, other authors proposed different solutions, replacing one axiom for another more suitable to a certain interpretation of justice in a bargaining system. The two typical alternatives are the Kalai-Smorodisnky [58] and the Kalai/Egalitarian solution [59]. The first proposes to substitute the IIR axiom for a Resource Monotonicity (RM) axiom, equalizing the ratios of maximal gains, and the latter proposes to drop the AFFINV axiom, proposing a solution that maximizes the minimum of surplus utilities.

Although considered as alternatives for the implementation in this text, as far as our literature review went, for the Kalai-Smorodinsky and egalitarian solution there is no n-th player solution applicable to the DVB implementation constraints, or similar implementations backed up by previous studies in the telecommunication scenario.

3.2 Introduction to Queueing Systems

Queue models are analyzed through the lenses of queueing theory, which is a branch of mathematics that studies the behavior of different types of lines/queues, having applications in many different fields and contexts. The main objective of this section is to introduce the necessary notation and definitions. Because we interpret that the overall resource allocation scheme for the RCSTs defines a queue, we take a brief look into the formulation of basic concepts so that the reader can follow the approach taken for the DVB-RCS2 MF-TDMA scheduler analysis.

It is believed that the beginning of the queue theory field started with A.K. Erlang, with a paper called “The Theory of Probabilities and Telephone Conversations” which was published in 1909. The main goal of Erlang was to define the number of telephone circuits necessary to guarantee a minimal waiting time for customers of its Copenhagen telephone company. He developed a mathematical framework that is applicable to many other fields, given that the idea of minimizing customer waiting time is useful for a number of different applications.

Many metrics can be observed and predicted through a queue analysis (e.g. average waiting time, average number of users in the queue, etc.). They are useful for network design. As users can enter the queue at random moments, the arrival is usually modeled as a Poisson distribution, and the average service depends on the capacity availability of the frame.

Complex input processes, service time distribution, and queue disciplines are all general queueing system characteristics. Complex queue systems are rarely accessible to analytical solutions in practice, as this analysis might have convoluted equations. Simple queueing models, on the other hand, can often provide insight and numerical tools to simulate and measure telecommunication traffic. This modeling simplification is often used in packet switching networks based on the store and forward concept, for example, such as the Internet. Packets traveling to their destinations typically arrive at a router, where they are stored and routed based on the addresses in their headers.

Explaining traffic behavior is important to justify implementation choices for telecommunication systems and to understand the impact of certain parameters on queueing performance, which is one of the goals of telecommunications research.

As described in the Survey [60]: "There has been an increasing interest in modeling and solving scheduling problems in dynamic environments. Such problems have also been considered in the field of queueing theory, but very few papers take advantage of developments in both areas, and literature surveys on dynamic sche-

duling usually make no mention of queueing approaches."So in this work we expand further the study of the connection between these two broad bodies of knowledge, one distinctive feature of this dissertation is the queue data gathering for the game theory scheduling algorithm. Daria Terekhov et al.[61] also display the importance of the integration between dynamic resource allocation and queue theory.

Before explaining the queue model used, we define the necessary tools and notations to tackle queue problems in general. There is a spotlight in probability theory elements that appear frequently throughout this work, although we assume a familiarity with probability, statistics, and stochastic processes on the reader's part.

3.2.1 Probability Review

Let X be a random variable and I its domain, we denote its probability density function as $P_X(x)$; $E[X] = \mu_X = \int_{x \in I} x P_X(x) dx$ is the average value of this variable, $var[X] = E[(X - \mu_X)^2]$ is the variance. We have that for every random variable the distribution $\int_{x \in I} P_X(x) dx = 1$. There are some key concepts that we chose to bring out as they are significant to this work proposed model formulation, these concepts are: Convolution, Poisson Distribution, Markov Chains, and stochastic matrices. The first one on the list, convolution, has an importance in the solution of the stochastic matrix that appear in our Markov chain model of the queue. We explain how this allows to calculate the stationary probability distribution, that is necessary to calculate queue parameters such as the average queue length of the system.

3.2.1.1 Queue Classification

To represent the type of queue we want to specify in a given context, a commonly used shorthand notation is used: Kendall's notation [62, p. 71]. It specifies the arrival process, service distribution, number of servers, and buffer size (waiting room) as follows:

Arrival procedure / service distribution / server count / waiting room.

In this notation, for the first two positions, the following characters are commonly used: D (Deterministic), M (Markovian - Poisson for the arrival process or exponential for the service period), G (General), GI (General and independent), and Geom (Geometric). The fourth position is used to provide the number of buffer seats in addition to the number of servers, and it is typically not utilized if the waiting room is unlimited.

M/M/1, for example, represents a single-server queue with a Poisson arrival mechanism and exponential service with an infinite buffer. M/G/k/k denotes an k-server queue with no additional waiting room except at the servers, with the arrival process being Poisson.

In this dissertation context we define the DVB-RCS2 MF-TDMA as a queue with Poisson entries, a predefined truncated Poisson service, a server count m which is a random variable per SF, and infinite waiting room.

3.2.1.2 Convolution

A concept that appears naturally when solving statistics and telecommunication problems [62, p. 12] is the convolution of two functions: let there be two functions $f, g : \mathbb{R} \to \mathbb{R}$, then the convolution is the function $f * g(x)$ defined as

$$(f * g)(x) = \int_{-\infty}^{\infty} f(\tau)g(x - \tau)d\tau, \tag{3.5}$$

and its discrete form, with discrete signals $f, g : \mathbb{Z} \to \mathbb{R}$, has the analogous definition

$$(f * g)[k] = \sum_{i} f[i]g[n - i]. \tag{3.6}$$

The Equation (3.6), with a geometric interpretation, means the area of the product of the two functions, where one is reflected and shifted by n to the right. If two signals have finite energy, the resultant convolution function has also finite energy.

In our scope of stochastic processes, we can define the convolution of random variables: let X_1 and X_2 be two independent random variables with probability density functions $P_{X_1}(x_1)$ and $P_{X_2}(x_2)$, then define a third random variable $Y = X_1 + X_2$, we can derive the probability density function $P_Y(y)$ of this variable as

$$\begin{aligned} P_Y(y) =& P((X_1 + X_2) = y) = \\ & \sum_{v} P(X_1 = v, X_2 = y - v) = \\ & \sum_{v} P_{X_1}(v)P_{X_2}(y - v). \end{aligned} \tag{3.7}$$

The Equation (3.7) has the form of the convolution of two functions as in Equation (3.6).

3.2.1.3 Poisson Distribution

When working with capacity request problems, we have to model the user's arrivals in the system. The users are terminals demanding capacity from the scheduler. One probability distribution function commonly used to define this type of

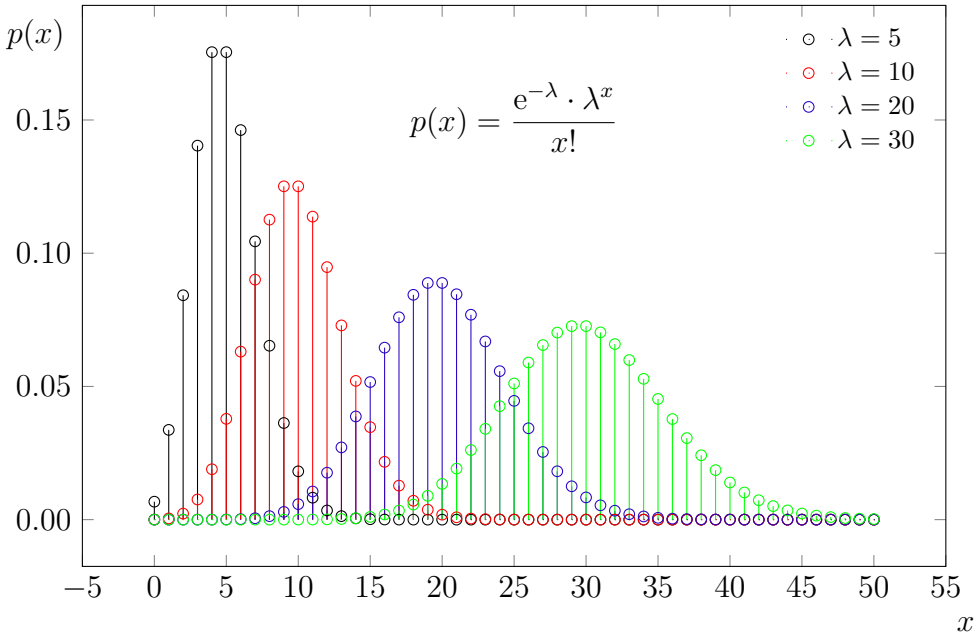

Figure 6 – Example of Poisson Distribution for different values of λ (Adapted from [63]).

arrival is the Poisson distribution. This function, in its core, is designed to spread the probability density such that the mean arrival rate per unit of time is λ, which is a chosen parameter of the distribution. Mathematically, as a function, the Poisson distribution is defined as

$$P_X(k;\lambda) = \frac{e^{-\lambda}\lambda^k}{k!}, \tag{3.8}$$

where k is the total number of arrivals in a given time frame and λ is the previously mentioned mean arrival rate, or in other words: $E[X] = \lambda$. Figure 6 shows the graph of the probability distribution for a Poisson distributed random variable, for different λ values.

Notice in Figure 6 that the graph has a positive skewness depending on λ, in fact $\text{skew}[x] = \lambda^{-1/2}$ and $var[X] = \lambda$. So in the limit, as the arrival rate grows, the distribution tends to a symmetric distribution.

3.2.1.4 Markov Chains

To begin discussing Makov chains we place some basic stochastic processes definitions:

Definition 3 *Let T be an index set, a* ***random process*** *is a collection of random variables $\{X_t, t \in T\}$. If each random variable in this collection is continuous/discrete we say that the random process is a* ***continuous/discrete space*** *stochastic process, if the index set T is continuous/discrete, we say that the stochastic process has* ***continuous/discrete time****.*

Certain stochastic systems can be fully described with the use of Markov-chains, a type of stochastic process that, among many applications, is widely used to simulate the behavior of discrete systems, such as traffic characterization, modeling of queues, and telecommunication networks.

In our context, we consider T as a set of time values. Let then be arbitrary times $\{t_1 < t_2 < \cdots < t_k < t_{k+1}\} \in T$. A Markov process X_t is a random process that has the following property: its future value at t_{k+1}, given the present time t_k, is independent of the past. This is the Markov property, expressed as

$$P\left(X_{t_{k+1}} = x_{k+1} | X_{t_k} = x_k, \cdots, X_{t_1} = x_1\right) = P\left(X_{t_{k+1}} = x_{k+1} | X_{t_k} = x_k\right). \quad (3.9)$$

Due to the fact that, in Markov processes, the probabilities can be conditioned only on the most recent time instant, the value of X_t at time t is called the state of the process at time t.

If a discrete-time stochastic process $\{X_n, n = 0, 1, 2, ...\}$ has the Markov property, that is, at any point in time n, its future state value is only dependent at its current state value and is independent of the past evolution of the process, we then call this process a discrete-time Markov-chain. We use a discrete-time Markov chain to model the timeslot resource allocation problem in the DVB-RCS2 return link. The DVB scheduling scheme is inherently discrete in time, as the allocation of an RCST is planned between two sequential SuperFrames, and as consequence, so are the RCSTs capacity requests.

The state of a Markov chain can be a scalar or a vector, but the scope of this work only ranges to scalar state Markov chain, as we use its states to track the number of RCSTs in the queue waiting to receive timeslots.

Finally, a time-homogeneous Markov-chain is a process in which

$$P(X_{n+1} = i \,|X_n = j) = P(X_n = i \,|X_{n-1} = j), \quad \forall n. \quad (3.10)$$

We will only consider Markov chains which are time-homogeneous. A discrete-time time-homogeneous Markov chain is then characterized by the property that, for any n, given X_n, the distribution of X_{n+1} is fully defined regardless of states that occur before time n.

3.2.1.5 Stochastic Matrices

We use analytical tools from probability theory and linear algebra to solve for the emerging properties of a given Markov chain, such as solving for the stationary probability vector of a stochastic process, i.e., the stationary probability distribution of the system being in a certain state. The probability of a transition between states of a Markov chain can be described in a condensed way by a probability transition matrix, also called a stochastic matrix. This matrix has many interesting properties, some of them required to understand the algorithms presented in further sections.

The entries of the probability transition matrix are

$$P_{ij} = P(X_{n+1} = j \mid X_n = i), \quad \forall n. \tag{3.11}$$

As we are considering a homogeneous Markov chain, the choice of n does not affect the conditional, so the definition (3.11) is not ambiguous. The rows of this probability transition matrix sum up to one, that is

$$\sum_{j=1}^{M} P_{ij} = 1. \tag{3.12}$$

M being the number of possible states in the Markov Chain. This class of matrices has an important property that the spectral radius is always 1, so its eigenvalues are always less or equal to one.

Given that the rows of this matrix sum up to 1, there is always a trivial right eigenvector with all entries equal to one $[1, 1, 1, 1 \ldots 1]$ and a trivial right eigenvalue 1. For square matrices, the left and right eigenvalues are equal; then, there is an associated left eigenvector for the eigenvalue 1. Furthermore, by the Brower fixed point theorem, as the matrix has spectral radius one, we can find this eigenvector by repeated iteration of the probability transition matrix operator, that is:

$$\lim_{k\to\infty} (P^k)_{ij} = \boldsymbol{\pi}_j, \tag{3.13}$$

where $\boldsymbol{\pi_j}$ is the j-th entry of this associated left eigenvalue, which we call stationary probability vector. Going back to our stochastic process context, this is a remarkable result. The iteration of the probability transition matrix, starting at any initial probability distribution vector, defines the conditional probability of the system being in a given state after n iterations of the process, that is

$$P^n_{ij} = P(X_n = j \mid X_0 = i), \tag{3.14}$$

Equation (3.13) then implies that no matter the initial distribution vector, there is an emergent probability vector after a long-time iteration. This result is fundamental

for queue analysis, as it allows a method for predicting the long-time behavior of a stochastic process. We use it to calculate the average waiting time in the queue and the average queue size.

In the next section we use these tools to build and analyze the Markov Chain queue model for the MF-TDMA capacity request DES framework.

CHAPTER 4

PROPOSED SYSTEM AND METHODOLOGY

4.1 Proposed DES Framework

A Discrete Event System (DES) implementation has a set of discrete states with an event-driven transition mechanism that triggers a state change to produce an output. Figure 7 shows a summary of the different classifications of systems, we see that DES defines a large portion of complex systems. If the original system to be modeled possesses a continuous-state behavior, its states smoothly change as time moves forward. However, when the original system is mapped to a DES implementation, only instantaneous transitions at predefined points in time need to be tracked. In this way, the simulation structure for an event-driven design requires a central scheduler to act as a bookkeeper and register all the event transition times in the model. As the events are asynchronous and may be concurrent, the register with the central scheduler must announce any changes within the set of states. Furthermore, other events can be affected by the state changes, so a list of scheduled events to be processed at any simulation step must be kept.

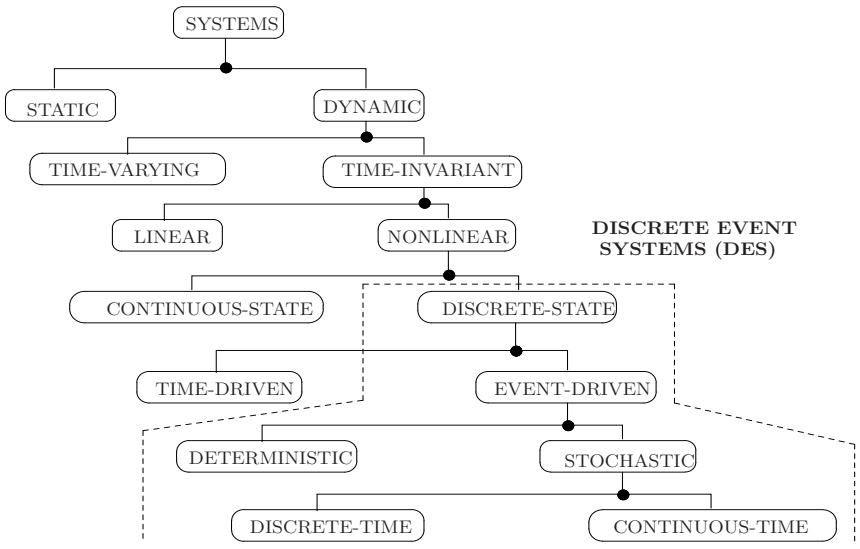

Figure 7 – Summary of systems classification, adapted from [64, p.46]

For the DES implementation, the state space X is a countable set of states s_i which is defined as:

$$X = \{s_1, s_2, \cdots, s_n, s_{n+1}, \cdots\}, \tag{4.1}$$

and a set of countable events E that consists of event e_i which is defined as:

$$E = \{e_1, e_2, \cdots, e_k, e_{k+1}, \cdots\}. \tag{4.2}$$

The time sequence of events to be processed is defined as a list L of pairs of events e_j and states t_i,which can be written as:

$$L = \{(e_1, t_1), (e_2, t_2), (e_3, t_3), \cdots\}. \tag{4.3}$$

Furthermore, the simulation runs in a way such that there is a time ordered scheduled event list L_s, with the smallest schedule time processed first. This way, the first event in the list is always the triggering event that produces the changes in the X set.

The mapping of these events and states in this framework was performed using the SimPy library [20], which implements event-driven behavior using the Python programming language. As Python allows for object-oriented programming, it creates a generator for each event that can be mapped to a function or a class method. This way, e_1 is mapped to a function that also defines the corresponding waking time t_1. Details of the implementation require that, in order to register, events share the same environment. This object also controls time sequencing.

The proposed simulator framework is presented in Figure 8. Text files contain input parameters related to the link nodes (RCSTs, satellite, NCC), channel modeling, MF-TDMA hierarchy, link-level performance curves, traffic profiles, antennas, and simulation campaigns. The event handling block that corresponds to the discrete-event simulation is described later in this section. During the simulation, each new superframe generates partial results in the output files. After the simulation reaches the end, the output files are post-processed to generate the plots indexed by load or simulation time. The simulator also provides geo-referenced results for an analysis of bandwidth utilization. Some of those results are shown and discussed in Section 5.1.

At the core of the simulator is a discrete event manager responsible for handling the dynamics of all connections in the network. SimPy was used as the discrete-event framework for the simulator implementation. For example, the SimPy framework handles multiple events related to the arrival and departure of RCSTs, their access to the network, and packet transmission. One important event is a possible packet collision in the Random Access (RA) pool during the logon procedure. In

particular, SimPy provides a `store` object [65], which is a FIFO (first-in, first-out) storage object that can trigger other processes whenever its contents are changed. The MF-TDMA structure follows the structure of Figure 13, where each channel in frequency is represented by one `store` object in memory. When a packet is inserted into the `store` object, which represents a packet being sent through the channel, the receiver process becomes awake (here modeling the NCC reception), handles the triggered event, and checks if more than one packet was received at the same time in order to detect collision.

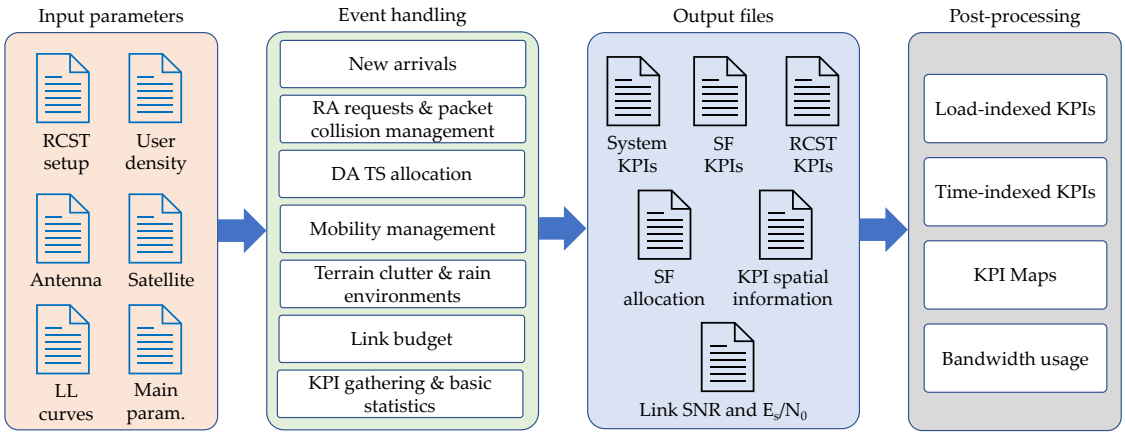

Figure 8 – General structure of the system-level simulator, with examples of input and output files. The event handling subsystem is responsible for RCSTs transmission management.

Figure 9 shows the life cycle of each user (or RCST) in the network, until it departures the queue. There are two possible ways that an RCST can enter the system, and once accepted, becomes part of the *active users* set. The first way is when the RCST is part of the initial load, defined by the simulation scenario setup. In this case, the RCST is already an active user. The second follows a Poisson probability distribution with an arrival rate λ generated at the start of each new SF. The arriving RCST needs to follow a logon process, which includes an attempt to get a resource from the RA pool. After a successful login (without collision with other RCSTs), an algorithm performs the proper TS allocation of the RSCT's data traffic at the Deterministic Access (DA) pool.

Each active user allocated in a SF has a data buffer to transmit. When an RCST transmits a packet, it is evaluated for packet error rates through a combination of a link budget procedure and a check of Es/N_0 requirements for the waveform used for transmission. All performance curves are obtained from an ex-

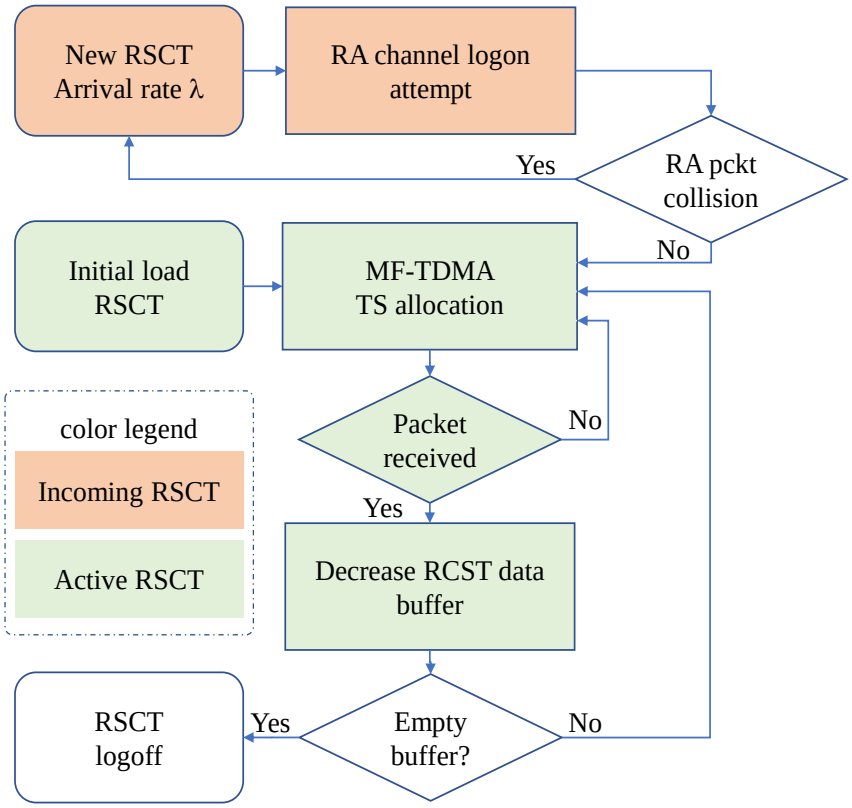

Figure 9 – Terminal lifecycle in the system. Optimization of resources within the RCS-2 MF-TDMA structure is performed at each superframe.

ternal link-level simulator [34] that handles the details of the channel coding and digital modulation for all ACMs in the standard documentation [7]. It is worth noting that link-level results affect system-level performance. From the perspective of the system-level simulator operation, link-level curves are tables retrieved at the beginning of the simulation. If changes in the receiver design affect the performance, the corresponding new tables can be replaced without changing the rest of the code. Also, it is possible to use the reference values for physical layer performance from [7, Sect. 10.2].

If a packet is successfully received, the total amount of data remaining in the RCST's buffer is decreased. If there is an error, the RCST retransmits the packet and maintains its active user status. When a new SF is created, the deterministic allocation algorithm handles the currently active RCSTs and all RCSTs that had their channel requests granted from the previous SF.

As the simulation continues to operate, output files with partial results are

produced. A set of key performance indicators (KPIs) were selected in this simulation framework to assist with the system performance analysis, such as latency due to the logon process, the number of frequencies used in the SF, the raw throughput at the PHY layer, and the goodput at the MAC layer. Results are collected for each RCST and for all SFs in the simulation. This allows for the post-processing and statistical analysis of the performance indicators.

4.2 DVB-RCS2 MF-TDMA system modeling

This section describes the modeling aspects of the DVB-RCS2 scheduling scheme implementation, focusing on the notation of necessary parameters and simplifying assumptions.

To simulate the birth and death of RCSTs, the ones attempting to enter the network are organized in a queue. Arrivals are modeled as a Poisson random variable, with parameter λ as the mean arrival rate per SF in the system. The λ parameter affects the system traffic intensity and the resource distribution performance.

Assigned to the i-th RCST ($i \in \{0, 1, \cdots, N-1\}$), there is a tuple of parameters: a volume of data V_i to deliver before leaving the system; a minimum required data rate to meet the QoS requirements d_i (in BTUs/s per SF); an expected data rate D_i (also in BTUs/s per SF); a burst length w_i (BTUs); an allocation priority p_i; and an information efficiency η_i (bits/symbol), defined in a finite set of waveform IDs summarized in Table 34. We also consider the time duration of an SF to be 1 second. This way, d_i and D_i are numerically equal to the number of BTUs allocated in an SF, while using the relative measurement of an SF period T_{SF} in BTUs/s.

An SF is modeled as a grid of $N_{SF} = T_{SF} \times K_{SF}$ BTUs. The i-th allocated RCST will receive ϕ_i BTUs per SF, no less than the minimum required d_i and no more than the expected D_i. The number of allocated users is determined by the maximum number of allowable RCSTs in an SF that still meet the minimum QoS requirement d_i. Assuming that an RCST can only use one frequency channel concurrently, the maximum resource allocation is limited by T_{SF} in the time domain of the SF.

The transmission is made through a specified MODCOD based on the link quality (E_s/N_0). The link quality defines the spectral density, so, even if the same number of BTUs are allocated to two different RCSTs, they will receive different amounts of information, given that they have different spectral densities. This difference is used by the proposed game theory algorithm to balance the fairness in the system.

Also, RCSTs are served in order of arrival: if an RCST is not allocated in the current SF, it maintains its position in the queue until eventually be served in the following SF.

The expected BTU rate D_i is modeled as $D_i = \alpha d_i$, where $\alpha \in [1, \alpha_{max}]$ is a truncated Gaussian random variable, with parameters (μ, σ) and $\alpha_{max} = T_{SF}/d_i$, which was a design choice to emulate a real case scenario, as the proposed algorithm performance depends on the dispersion of the D_i distribution. The α_{max} value is such that the expected BTU rate does not surpass the maximum possible allocation in an ACM channel. This formulation models a random data demand of bandwidth by the terminals. Parameter α has distribution

$$p(\alpha) = \begin{cases} \dfrac{1}{\hat{p}\sqrt{2\pi}\sigma} \exp\left[-\dfrac{(\alpha-\mu)^2}{2\sigma^2}\right], & 1 \leq \alpha \leq \alpha_{\max}, \\ 0, \quad \text{otherwise}, \end{cases} \tag{4.4}$$

where $\hat{p}$ is a normalization factor such that $\int_1^{\alpha_{\max}} p(\alpha) d\alpha = 1$. With this truncation, in general $E[\alpha] = \bar{\alpha} \neq \mu$, but we have considered a range of values μ and σ such that the difference can be disregarded.

We also consider the total useful information per BTU

$$q_i = \eta_i \times T_{\text{BTU}} \tag{4.5}$$

in bits per BTU, where T_{BTU} is the length of a BTU in symbols. The value q_i is the amount of allocated BTUs that carries data information bits, disregarding control/redundancy bits. The information payload of the allocation is thus $\phi_i^* = q_i \phi_i$, as depicted in Figure 10.

Figure 11 represents the probability distribution of the random variable D_i to each RCST, under this model.

When we take into account all the RCSTs, we define the allocated resource distribution vector in an SF as

$$\boldsymbol{\phi} \triangleq (\phi_0, \phi_1, \cdots, \phi_{N-1}), \ \ \phi_i \in \mathbb{R} \geq 0. \tag{4.6}$$

Figure 12 illustrates the SF when filled by $\boldsymbol{\phi}$. The ϕ_i allocated to an RCST is always a multiple N_i of the BTU size T_{BTU}. In frequency, it occupies a fixed multiple L_i of the BTU bandwidth B_{BTU}.

The fairness of an allocation can be measured with the Jain fairness index [66]

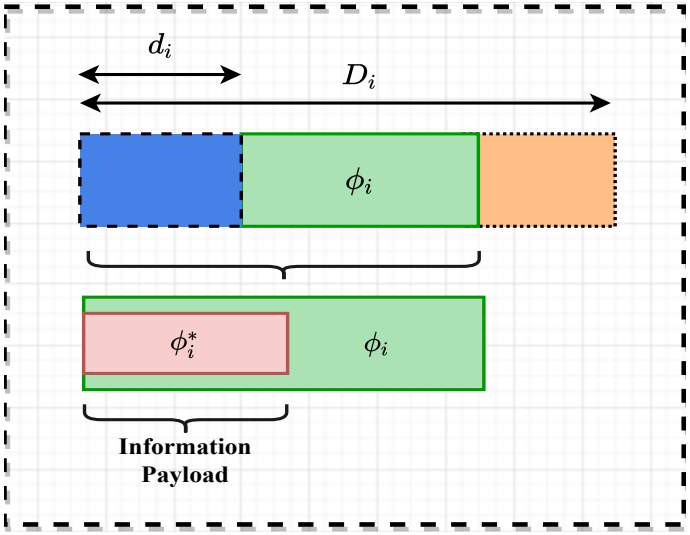

Figure 10 – Allocation range (d_i, D_i) and the information payload ϕ_i^* in a TS.

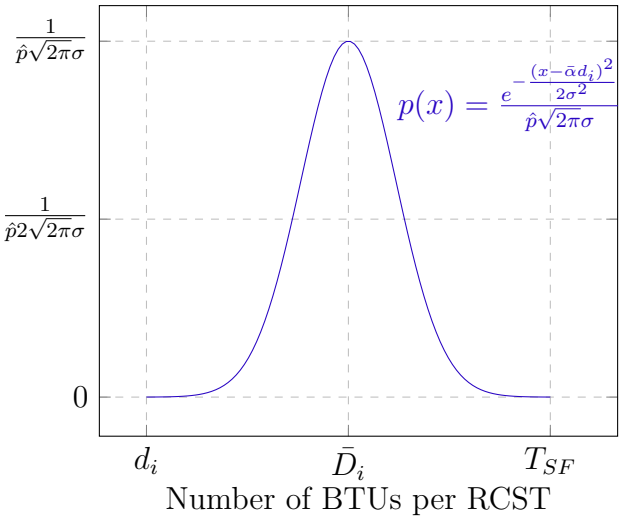

Figure 11 – Expected BTUs probability density distribution for each RCST.

$$J(\boldsymbol{\phi}) = \frac{\left(\sum_{i=0}^{N-1} \frac{\phi_i}{D_i}\right)^2}{N \sum_{i=0}^{N-1} \left(\frac{\phi_i}{D_i}\right)^2} = \frac{\left(\sum_{i=0}^{N-1} \hat{\phi}_i\right)^2}{N \sum_{i=0}^{N-1} \hat{\phi}_i{}^2}, \tag{4.7}$$

where $\hat{\phi}_i = \frac{\phi_i}{D_i}$, the normalized BTU distribution, is the ratio between the capacity an RCST receives and the capacity it requests. $\hat{\phi}_i$ can be interpreted as a measurement of the satisfaction an RCST experiences after receiving ϕ_i BTUs from the NCC's scheduler. The Jain fairness index measures then the perceived average fairness of the resource allocation, and it is dependent on the coefficient of variation of a given

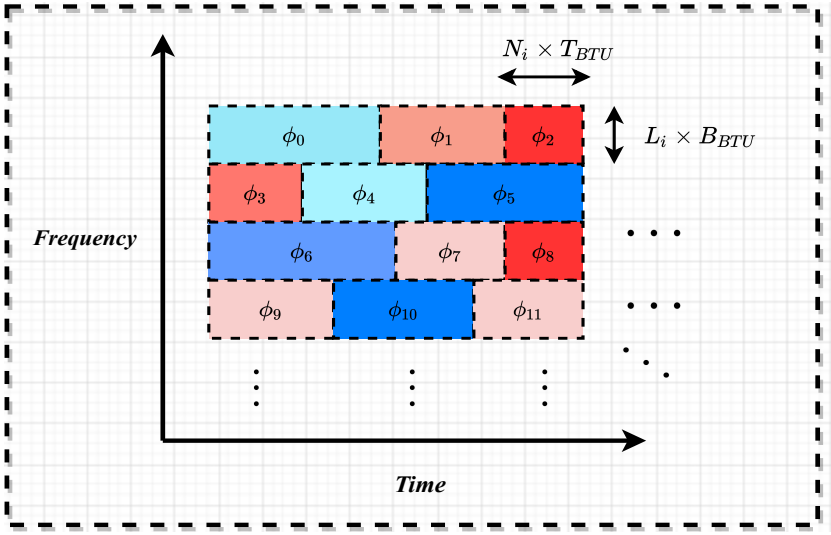

Figure 12 – Distribution of BTU resources ϕ_i in a DVB-RCS2 SF. All ϕ_i occupies the same bandwidth in an SF.

distribution vector. There is a large body of literature about fairness metrics [67] and different ways to construct a custom fairness measure [68] to highlight certain aspects of a given distribution. We chose the Jain index as the benchmark fairness metric as a means to suit with past analysis of the game theory bargaining solution for resource allocation in a satellite communication system.

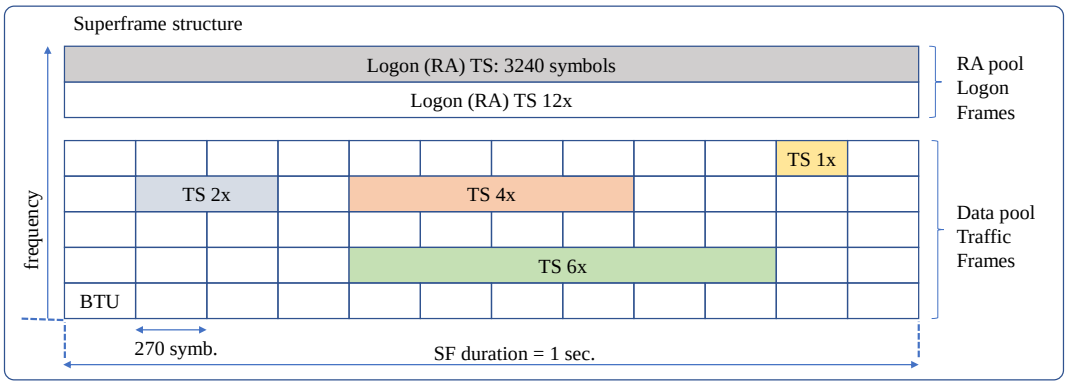

Figure 13 – Organization of the MF-TDMA hierarchy in the simulator (SF, frame, TS and BTU) with two pools of channels: RA for signaling and DA for traffic data. All logon messages use 12 BTUs as a worst case for Waveform 41 in Table 10.4 in [7]. The data BTUs are dynamically allocated, based on current E_s/N_0 and and recommended waveforms, both obtained from link level simulations.

Figure 13 illustrates a simplified view of the MF-TDMA, which the proposed simulator employs. In this figure the RA pool consists of logon frames represented

by incoming RCST login requests. The DA pool corresponds to the RCST data traffic frames. Inside a DA pool, the packet scheduler is active and performs the TS allocation procedure defined by the algorithms described in Section 5.1. The burst lengths are 266, 536, 1616, and 3236 symbols. Adding four symbols as guard symbols result in TS lengths of (respectively) 270, 540, 1620, and 3240 symbols, all multiples of 270 (1x, 2x, 6x, and 12x). The largest (12x) is also selected to carry random access (RA) signaling, as the standard assigns it to the most robust ACMs.

4.2.1 SDA and GPA Algorithms

To assess the resource allocation functionality in the event-driven system-level simulation software, we implemented simple versions of the CRA and FCA mechanisms, explained in Section 2.5.1. The experimental observations of these algorithms later inspired the introduction of the Min/Max and the Game Theory algorithms, used to further analyze the queueing trade-offs that appear in the studied scheduling scenarios.

For the CRA mechanism, we chose an algorithm based on a greedy strategy, referred to in this work as the Greedy Priority Allocation (GPA). It is defined in Algorithm 1. It traverses the SF DA pool sequentially, allocating at each step the necessary timeslot length to meet the RCST's QoS requirements. The allocation continues until the exhaustion of SF resources. Assuming an agreed data rate R_i to the RCST i and defining $T_{SF} = 1$ second, the necessary timeslot length d_i (in BTUs) can be calculated as:

$$d_i = \left\lceil \frac{R_i}{P_i} \right\rceil B_i, \tag{4.8}$$

where P_i is the payload in the ACM of the RCST, which is a function of its E_s/N_0 in the return link connection. B_i is the value of BTUs per burst, an integer value, which is also referred to as the BTUs per waveform, with $T_{SF} = 1$ the unit of R_i is given by SF.

Algorithm 1 describes the procedure for the GPA algorithm. While there are BTUs available in a Superframe (SF BTUs) and a feasible DRA channel available (DRA $k \leq K_{\mathrm{SF}}$) the GPA algorithm must inspect if allocating the current RCST i is feasible. In case of a true condition, the RCST must be allocated, and the utilized BTUs must be subtracted from the total available. The final step is to attend to the next RCST in the queue. In case of false condition, GPA algorithm skip to the next DRA channel and reiterate.

The allocation procedure also prioritizes users according to their SNR. RCSTs with a larger SNR will be served first, in contrast to the RCSTs with lower SNR,

Algorithm 1 GPA - Greedy Priority Allocation

```
Sort RCST queue based on SNR
while SF BTUs > 0 and DRA k ≤ K_SF do
    if (DRA k BTUs − D_i) ≥ 0 then
        Allocate D_i to RCST i
        Subtract D_i BTUs from DRA k and from SF
        Go to next RCST i + 1
    else
        Go to next DRA k + 1
    end if
end while
```

which typically need a more significant portion of the SF in order to complete their QoS requirements, in terms of Jain fairness, this allocation is maximally fair per SF, but we see that the implications of this priority queueing affects other trade-offs in the total queueing system.

To verify the simulator predictions in an FCA allocation context, we employed an algorithm that equally divides the surplus capacity between each RCST. In this algorithm, denoted by Simple Division Algorithm (SDA), which is presented in Algorithm 2, the scheduler equally divides the number of BTUs in an SF to each RCST. This strategy is not a greedy one, as it needs the information of all RCSTs in the queue to perform the resource allocation. If any of those RCSTs do not meet their minimum data rate requirement, then the least element in the RCST list is temporarily discarded to be allocated in the next Superframe. This process repeats until all RCSTs meet their minimum data rate requirements.

Algorithm 2 explains the SDA algorithm operation. The total number of BTUs in a SuperFrame (SF BTUs) is divided by the total number of RCSTs to be served (N). This variable is denoted as Div. It must be verified whether Div is greater than all RCSTs' required timeslots (TS_i), *i.e.* whether all RCSTs receive more BTUs than the minimum to satisfy their minimum data rate requirements. If this is the case, Div as a multiple of the waveform length in BTUs must be allocated to each RCST. Otherwise, one less RCST should be served, the last one in the queue, and the algorithm is reiterated until all allocated RCSTs satisfy the minimum data rate requirements.

4.3 The Proposed Bargaining Solution

Interpreting the RCST resource scheduling dilemma as a game theory bargaining problem, each ϕ_i in Equation (4.6) is understood as a utility function. To solve

Algorithm 2 SDA - Simple Division Allocation

1: $Div = SF\ BTUs/N$
2: **while** (any $TS_i - Div) < 0$ **do**
3: Pop last RCST in the RCSTs list
4: Decrement N
5: $Div = SF\ BTUs/N$
6: **end while**
7: Allocate to each RCST Div as a multiple of the waveform length in BTUs.

this bargaining problem the Nash bargaining solution is employed. The objective function for the weighted Nash bargaining solution is

$$\mathcal{N}_B(\boldsymbol{\phi}, \boldsymbol{p}) = \prod_{i=0}^{N-1} \phi_i^{p_i}, \tag{4.9}$$

where p_i is a priority weight ascribed to each RCST. A larger p_i means a higher priority in the allocation i.e., more BTUs proportionally to the other RCSTs at the optimal assignment.

It is possible to modify the objective function (4.9) into a concave function by employing a logarithmic transformation, and thus the problem become a convex optimization problem. The full statement using the defined variables therefore becomes

$$\max_{\boldsymbol{\phi}} \sum_{i=0}^{N-1} p_i \ln \phi_i \tag{4.10}$$

$$\text{s.t. } \phi_i \leq D_i \quad \forall i, \tag{4.11}$$

$$\phi_i \geq d_i \quad \forall i, \tag{4.12}$$

$$\phi_i \geq 0 \quad \forall i, \tag{4.13}$$

$$\sum_{i=0}^{N-1} \phi_i \leq N_{SF}. \tag{4.14}$$

Employing the method of Lagrange multipliers, the Lagrangian function for Equation (4.10) can be written as

$$\begin{aligned} \mathcal{L}(\boldsymbol{\phi}) = \sum_i p_i \ln \phi_i + \kappa \left(N_{SF} - \sum_{i=0}^{N-1} \phi_i \right) \\ + \sum_i k_i(\phi_i - d_i) + \sum_i K_i(D_i - \phi_i), \end{aligned} \tag{4.15}$$

where κ, k_i and K_i are non-negative Lagrange multipliers. The choice for ϕ_i is optimal when $\frac{\partial \mathcal{L}}{\partial \phi_i} = 0$, that is

$$\frac{\partial \mathcal{L}(\boldsymbol{\phi})}{\partial \phi_i} = 0 = \frac{p_i}{\phi_i} - \kappa + k_i - K_i, \tag{4.16}$$

with the Karush–Kuhn–Tucker (KKT) conditions, that results from the inequality constraints in Equation (4.10), being

$$k_i(d_i - \phi_i) = 0, \tag{4.17}$$

$$K_i(D_i - \phi_i) = 0. \tag{4.18}$$

From conditions (4.18) applied in (4.16) and solving for ϕ_i following the steps at [23, 24], we get

$$\phi_i = \begin{cases} p_i\upsilon, & \text{if } \; d_i < p_i\upsilon < D_i, \\ d_i, & \text{if } \; p_i\upsilon \leq d_i, \\ D_i, & \text{if } \; D_i \leq p_i\upsilon, \end{cases} \tag{4.19}$$

where $\upsilon = 1/\kappa$ is a chosen constant such that the constraint $\sum_{i=0}^{N-1} \phi_i \leq N_{SF}$ is met. This solution resembles the solution for the water filling problems [69, 70] that often appears in wireless communication papers.

We propose to define the priority weights in the general Nash bargaining solution convex problem formulation (4.10) as $p_i = 1/q_i$, where q_i is the total useful information payload per BTU, defined previously in (4.5). This modification changes the solution so that the algorithm considers the useful capacity gained by an RCST, with every BTU, knowing that an RCST with a higher SNIR has a larger information payload per burst and thus gains more utility per BTU.

This modification guarantees an overall fairer approach, as the legacy solution with all equal priorities allocates the surplus equitably in terms of BTUs but not in terms of endpoint capacity that an RCST receives.

Notice that although (4.10) is a real convex optimization problem, meaning it can output solutions in all $\mathbb{R}^+$, the solution in the DVB-RCS2 SF demands an integer allocation, ϕ_i must also be a multiple of the burst length ω_i.

An integer solution can be obtained with a rounding process described in [24], where the fractional part of each ϕ_i is added i.e.

$$\phi_{\text{freed}} = \lfloor \sum_{i=0}^{N-1} (\phi_i - \lfloor \phi_i \rfloor) \rfloor, \tag{4.20}$$

where $\lfloor . \rfloor$ is the floor function and ϕ_{freed} is distributed to each RCSTs in order of priority p_i, a burst length w_i at a time to each RCST, until all BTUs are allocated. As the amount of resources allocated are way larger than ϕ_{freed}, the loss in optimality by this rounding process is minimal and thus can be disregarded.

4.4 Proposed DVB-RCS2 MF-TDMA Queueing Model

The RCSTs arrive to be served. They position themselves in an ordered queue. Each RCST makes a Rate-Based Capacity Request (RBCR), expecting to have this rate fulfilled by the scheduler, receiving BTUs in the SF. There is only a limited number of BTUs per SF, so the BTU resource must be allocated strategically in order to maximize allocation satisfaction. In this context, this means how much of the expected rate a given RCST has received. We also want to minimize service delay, maximize fairness, and other queue parameters, such as average departure rate and average service rate (which translates to average throughput).

A minimum data rate is guaranteed for each RCST that is allocated in the current SF. If there is enough BTUs to serve the minimum service to each RCST, then the surplus capacity is allocated in a fair manner through the bargaining solution algorithm, guaranteeing proportional fairness and Pareto efficiency. If not possible to allocate every RCST that arrived in the frame, this RCST will remain in the queue for the next SF. Each RCST has a given number of bytes to be served B_l by the system until it departs. The scheduler will not allocate to each RCST more than its expected value at each SF.

The variables are labeled in Table 3, the strategy here is to think of this system as a multi-server queue, that is, a queue with m servers with Poisson arrivals and an average minimum service rate μ. We have to treat m as a random variable and study the emergent properties of this value once the queue stabilizes. This μ can be modeled as the average minimum service in BTUs, then the number of servers m is the quantity of μ slots that fits in an SF.

Table 3 – Table of Queue Parameters

Symbol	Description
λ	Mean number of RCSTs arrivals per SF
ρ	Traffic intensity of the system
μ	Average service rate
B_L	Buffer length
P_q	The probability that an arriving terminal has to wait in queue
N	Average number of costumers waiting in the system
T_{ts}	Average time until served, waiting in queue
T_{th}	Maximum waiting time threshold
N_{SF}	Number of BTUs in an SF

Define $P_{d_i}(x)$ to be the probability density function of the random variable d_i, which is the length in BTUs of the minimum service in an arriving RCST, let

$\mu = E[d_i]$ and $m = \frac{N_{\text{SF}}}{\mu}$, where N_{SF} is the total number of BTUs in the SF. Define $\rho = \frac{E[B_L]\lambda}{m\mu}$ as the traffic intensity, where B_L is a random variable that represents the buffer length of the RCST, i.e., the amount of BTUs to receive until the service is complete.

Every equation here is described as a function of the variable m, the reason behind it is that m is a variable controllable by the scheduler. As a consequence of our construction, μ is also a controllable variable. Both ρ and λ are dynamic parameters of the queue, so they are not in control of the scheduler.

Denote $P_{\alpha X}(x)$ as the probability density function of the minimum service to an RCST multiplied by a real parameter $\alpha \in [1, \infty)$, then $\mu_\alpha = E[\alpha X] = \alpha E[X] = \alpha\mu$, so $m(\alpha) = \frac{N_{\text{SF}}}{\alpha\mu}$. Controlling the parameter α in the scheduler, we can control the queue behavior to some extent, as the parameters ρ, λ and the allocation of resources dictates the behavior of the queue system.

We want to model the DVB-RCS2 scheduling system as a queue using Markov chain, so it is necessary to model the states and the probability transition matrix. The Markov states in this formulation are defined as the number of RCSTs active in the system waiting for BTUs, so the final steady state distribution gives us information on how many terminals to expect in the system on average at each SF.

Let A be the random variable that represents the number of arrivals, we will model A as a Poisson distributed random variable, or $A \sim P_A(k, \lambda)$. Because the probability of arrivals in the queue is independent of the current state of the system, the average arrival is modeled by the Poisson parameter λ, measured in RCSTs per SF. We will shorten the notations using $a_i = P[A = i]$.

Let C denote the number of RCSTs completed in a given SF. The probability distribution of C depends on the number of RCSTs currently allocated in the frame, i.e, it depends on the state of the Markov chain at the given moment of evaluation. The distribution of C becomes independent of the state once the number of RCSTs allocated in the system is sufficiently large and the SF reaches its allocation capacity. The C random variable distribution will be denoted as $P_C^k(i)$, which represents the probability distribution that i RCSTs are completed when the system is in state k, indicating that $(k-i)$ RCTs will remain in the system. If $k \geq m$, then $P_C^k(i) = P_C^m(i)$.

When the system is in state k, the probability that it will transition to state $k + j$ is the probability that the difference between the number of RCST arrivals

and the number of RCST completions results in a net value of j RCSTs, or

$$P_{k,k+j} = P_C^k(0)a_j + P_C^k(1)a_{j+1} + P_C^k(2)a_{j+2}\cdots = \sum_{i=0}^{\infty} P_C^k(i)a_{j+i}. \tag{4.21}$$

With this result we can define the state transition matrix of this Markov system. The transition matrix being defined as

$$\mathbf{P} = \begin{bmatrix} P_{0,0} & P_{0,0+1} & P_{0,0+2} & \dots \\ P_{1,1-1} & P_{1,1} & P_{1,1+1} & \dots \\ P_{2,2-2} & P_{2,2-1} & P_{2,2} & \dots \\ \vdots & \vdots & \vdots & \ddots \end{bmatrix}, \tag{4.22}$$

where $a_{-j} = 0,\ \forall j > 0$ and $P_C^k(i) = 0,\ \forall i > \min(k, m)$.

Based on queue simulations made with the proposed DES structure described, we made a proper *Ad hoc* approximation for $P_C^k(i)$, we defined it as

$$P_C^k(i) = \frac{e^{-m\mu}(m\mu)^i}{i!\beta}, \quad 0 \le i \le \min(k, m). \tag{4.23}$$

Where β is a normalizing constant such that $\sum P_C^k(i) = 1$.

Better definitions for $P_C^k(i)$ may be obtained analytically, but the search for the exact solution to this distribution ended up being out of the scope of this text. It would be possible to employ a similar strategy as P.D. Mitchell [71], where the author discovers an analytical model for the Round-Robin scheduling for a geostationary satellite system, in our model, to compute the numerical approximations, we truncate the maximum number of RCSTs in the queue to a predetermined value. This is a valid approximation as states with a higher order get more improbable in proportion to the frame capacity, assuming a stable queue.

The choice of $P_C^k(i)$ is necessary to simulate the Markov Chain to find the stationary probability vector $\boldsymbol{\pi}$, therefore being able to calculate the queue parameters of interest. Given a state transition matrix, we can find the stationary probability numerically. We can either find the eigenvector of the state transition matrix for the eigenvalue 1 or apply another more efficient and sophisticated method. In the first case, the eigenvector can be found by repeated iteration of multiplying P with itself, for example.

Notice that (4.21) is a convolution (3.6) (or correlation, in another perspective) of the distribution $P_C^k(i)$ and a_i (flipped), and that (4.22) is approximately a Toeplitz matrix, that is, a matrix where the rows are just shifts of the previous row. This could imply simplifications in the calculation of the eigenvectors (i.e. the

stationary probability) analytically, using some known relationships between the Toeplitz matrix eingenvectors and the Fourier transform. But then again, the diving into these more convoluted analytical aspects were omitted from this work, to not diverge from scope, giving margin to a future work.

Having the stationary distribution vector $\boldsymbol{\pi}$, we can calculate the average number of waiting RCSTs in the queue by

$$N_Q(\boldsymbol{\pi}) = \sum_{m}^{\infty}(i-m)\pi_i = \sum_{0}^{\infty}(i)\pi_{i+m}, \tag{4.24}$$

that is, not accounting the states in which the RCST can be served by the m servers, the average state the system will be. By Little's formula, we can use this relationship to find the average waiting time-until-served using the relationship

$$T(\boldsymbol{\pi}) = \frac{N_Q(\boldsymbol{\pi})}{\lambda}, \tag{4.25}$$

where λ is the average arrival of RCSTs, discussed previously. We used a least squares fitting function in the Scipy optimize module for the numerical time-until-served predictions in the event-driven simulator, as simulating the Markov Chain at each iteration of an SF was computationally demanding. We based ourselves on an expected behavior analogous to the well-known formula for the continuous time M/M/m formula, fitting the equation

$$T_\alpha(\rho) = \frac{a}{1-\rho} + b\rho + c, \tag{4.26}$$

and finding the coefficients a, b and c for a sufficient range of α values, based on the simulation scenario. This base equation was chosen as it meets the divergent behavior when $\rho \to 1$ and closely fits the simulation results.

As a basis for our experiments, we analyzed our model compared to two contrasting allocation scenarios: the allocation policy where the scheduler allocates only the minimum of BTUs allowed to each RCST (*Min Alloc*, described in Algorithm 3), and the policy where the scheduler allocates all the BTUs from the RCST expected request (*Max Alloc*). For the sake of completion and data gathering, we also analyzed the behavior of the game theory algorithm in these same scenarios.

To extend the knowledge developed here, we propose the GTAC Algorithm 4, which switches to a more active perspective and attempts to control the queue with a predictive model based on traffic intensity. It keeps the average time-until-served at a stable threshold controlling the α value of the scheduling. This allows us to control the Throughput/Time Until Served trade-off, this behavior is explained in the results section. .

Algorithm 3 Min (Max) Alloc - Minimum (Maximum) Request Allocation Algorithm

Input: N_{SF}, d_i (D_i for Max Alloc) , $\forall i$,
Output: ϕ_i, $\forall i$.
while $N_{SF} > 0$ and DRA $k \leq K_{\text{SF}}$ **do**
  if [DRA k BTUs $-d_i$ (D_i)] ≥ 0 **then**
    Allocate d_i (D_i) to RCST i
    Subtract d_i (D_i) from DRA k BTUs and N_{SF}
    Go to next RCST $i+1$
  else
    Go to next DRA $k+1$
  end if
end while

Algorithm 4 GTAC - Game Theory Alpha Controlled Allocation Algorithm

Input: N_{SF}, d_i, D_i, ρ and T_{th}, $\forall i$,
Output: ϕ_i, $\forall i$.
Use time until served model matrix to find α such that $T(\rho) = T_{th}$
while $N_{SF} > 0$ and DRA $k \leq K_{\text{SF}}$ **do**
  if [DRA k BTUs $-\phi_i$] ≥ 0 **then**
    Allocate $\phi_i = \min(\alpha d_i, D_i)$ to RCST i
    Subtract ϕ_i from DRA k BTUs and N_{SF}
    Go to next RCST $i+1$
  else
    Go to next DRA $k+1$
  end if
end while
if $N_{SF} > 0$ **then**
  Run game theory algorithm in the remaining resource BTUs.
  $\phi_i = \phi_i +$ Surplus BTUs from bargaining solution.
end if

The GTAC algorithm differs from the other algorithms explained in this text in two ways: Firstly, we must feed the algorithm with the ρ value at each iteration, meaning that the scheduler must be able to keep track of the statistics of the RCSTs requests. This value must be calculated at each SF iteration. Secondly, T_{th} is a threshold value for the system's average time until served, which must be chosen by the system's designer.

The algorithm uses the Markov Chain model to try and "follow" the waiting time threshold value. It uses the maximum α value such that the time threshold is satisfied for a given ρ. We find the maximum α using the $T_\alpha(\rho)$ model prediction. When this procedure is finished, the algorithm uses the NBS to share the surplus BTUs (if any) in a fair manner.

In the next section we explain the results achieved from this algorithm and the possible implications it might have for future work.

CHAPTER 5

SYSTEM PERFORMANCE

5.1 DES Proposed Framework Simulation Results

Through the use of the proposed simulation framework, which was designed to analyze and evaluate solutions for problems that appear when performing planning and scaling activities in satellite networks, proposed use cases are described below.

We implemented two different algorithms to assess multi-user scheduling and allocation within the RCS2 MF-TDMA structure to provide a comparative study. The optimal resource allocation problem for the reverse link multiple access is investigated thoroughly in the academic literature [24, 23, 14], although it is rarely analyzed through the entire DVB-S2X/DVB-RCS2 system pipeline, with a realistic link performance, request queues, and spatial distribution for the RCSTs. In this case, we addressed all of these within the constraints of the ETSI RCS2 standards [72, 6, 73], which implied a need for a detailed evaluation of link performance for each user in the spatial dimension. End-to-end link quality is affected by the channel conditions and satellite footprint, both of which are functions of space. Hence, the use of maps and location coordinates, which is particularly relevant to satellite communications, was considered in this study. The last problem that was addressed focused on the spectrum allocation decision; namely, the amount of frequency allocated for both login and traffic channels, and how this proportion would affect the global behavior of the network.

We considered values of mobile users traffic demands from low to moderate data rates (below 100 kbits/s). The chosen geographical area was the entire country of Brazil, since it possesses the following features: (i) its geographical extension, suited to be covered by the footprint of GEO satellites; (ii) its span of different climate zones, which include both rainy and dry regions; and (iii) the uneven spatial distribution of its population, which has a higher density in the littoral coast and the south/southeast areas. Figure 14 depicts a cellular coverage map of Brazil that verifies a concentration of available wireless services in the regions mentioned above.

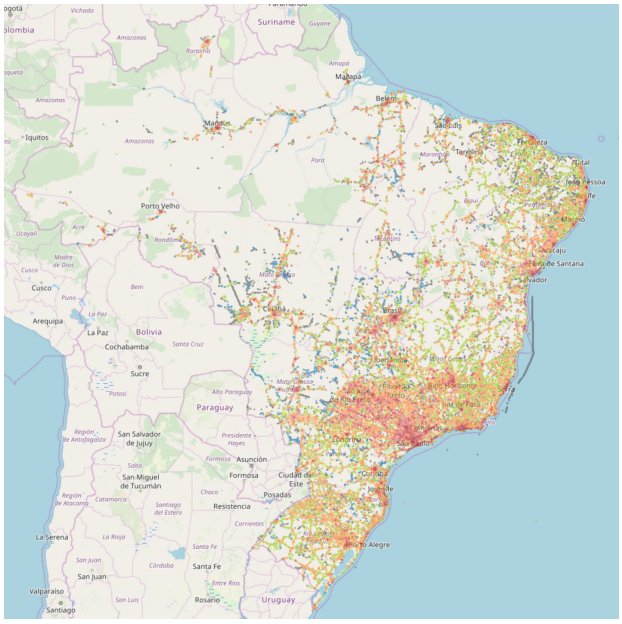

Figure 14 – Typical cellular coverage in Brazil. Users are mainly located along the coastline and in the southeast region of the nation (adapted from [74]).

The features of the simulator are evaluated through an analysis of the satellite network behavior in three cases: (i) choice of the allocation algorithm, (ii) results displayed spatially over a geographical territory, and (iii) bandwidth requirements for RA and DA pools. The scenarios of simulation were implemented focusing in a typical fleet tracking application scope, each simulation scenario was mainly defined by the initial RCSTs in the system and the arrival rate λ of new ones. Other system parameters with fixed values within the scope of this dissertation are presented in Table 4.

Table 4 – Parameters used in the system-level simulations.

Parameter	Value	Unit
Simulation time	25	seconds
Superframe duration	1	second
Bandwidth per BTU	150	kHz
Minimum RCST data rate	10	kbits/s
RCST buffer size	10	kbytes
DA pool bandwidth	900	kHz
RA pool bandwidth	600	kHz

5.1.1 SDA and GPA Algorithm Comparison

The first application example that was chosen to show the features of the system level simulator was to evaluate the impact of using distinct user allocation algorithms and verify how those strategies influence the overall network performance. We implemented the GPA and SDA algorithms to evaluate the simulator predictions of network behavior in a DVB-S2X/DVB-RCS2 compliant scenario.

Each load point $N_{U,t}$ is the average number of RCSTs entries in the network. In a simulation, $N_{U,t}$ is defined by:

$$N_{U,t} = N_{U,0} + \lambda T_{sim}, \tag{5.1}$$

where $N_{U,0}$ is the initial number of users, λ is the arrival rate, and T_{sim} is the value of simulation time taken from Table 4. Here we addressed the effect of changing $N_{U,0}$ and λ of new users according to Table 5. The set of results found with these experiments explores the Q1 in Section 1.4. For both options of the allocation algorithms, and for different loads, Figure 15 shows that the total throughput was similar per SF regardless of the allocation algorithm.

Table 5 – Load points for simulation scenarios.

Parameter	Initial value	Step	Final value
$N_{U,0}$	100	100	400
λ	10	20	70

However, it is possible to verify from Figure 16 a difference between GPA and SDA when the average throughput per RCST is considered. While the GPA algorithm attempted to maintain the data rate transmission of 10 kbits/s for each user, the SDA algorithm used spare BTUs to increase individual data rates. On the other hand, as the load increased, unused resources in an SF gradually disappeared, and the SDA algorithm could not make use of them.

There was also a second impact on the network performance if the dynamic behavior of active RCSTs in the system is considered. As each RCST had a buffer with data to transmit, there were differences in the time needed to empty them. As shown in Figure 17, this time duration was shorter when using the SDA algorithm when compared to the GPA algorithm. As a global result, there was a better dynamic utilization of the DA pool.

Another way of interpreting this result is by observing Figure 18. In this case, simulations showed that the average number of active users in an SF was different for both cases. The Figure 18 shows that for the GPA algorithm there were more

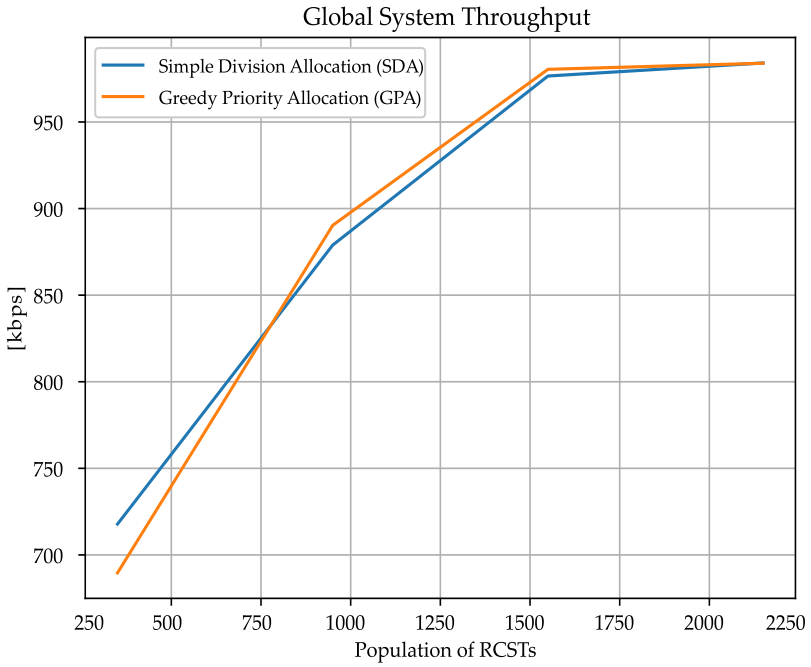

Figure 15 – Global throughput of GPA and SDA allocation algorithms for different load points.

users when compared to the SDA algorithm, but they remained in the system for a longer time, as Figure 17 shows. This result reinforces the need for a policy of load management that uses the flexibility of dynamical allocation of the RCS2 standard and the admission policy of new users. Finally, while the GPA algorithm allows for a distribution that will always satisfy the predefined rate requirements, it may also waste bandwidth capacity as it only allocates the necessary amount of BTUs to each RCST. This effect was most evident in scenarios with low values of the rate of arrivals λ.

5.1.2 Geospatial Network Performance Results

Beyond the statistics obtained from the MF-TDMA structure, the simulator displayed spatial results. The simulator produced the geographical information by calculating the link budget for each point on the map. The complete calculation required information about the transmitter, receiver, channel impairments, and noise, such as transmitted power; the position of the satellite (which in this case was geostationary); the channel modeling (free path loss and troposphere effects); and the main characteristics of the antennas used on link endpoints (NCC and RCSTs), namely the antenna gains G and their effective noise temperature T. For the satellite antenna, it was also possible to use the G/T footprint for the coverage area, as G and T were not always separately available.

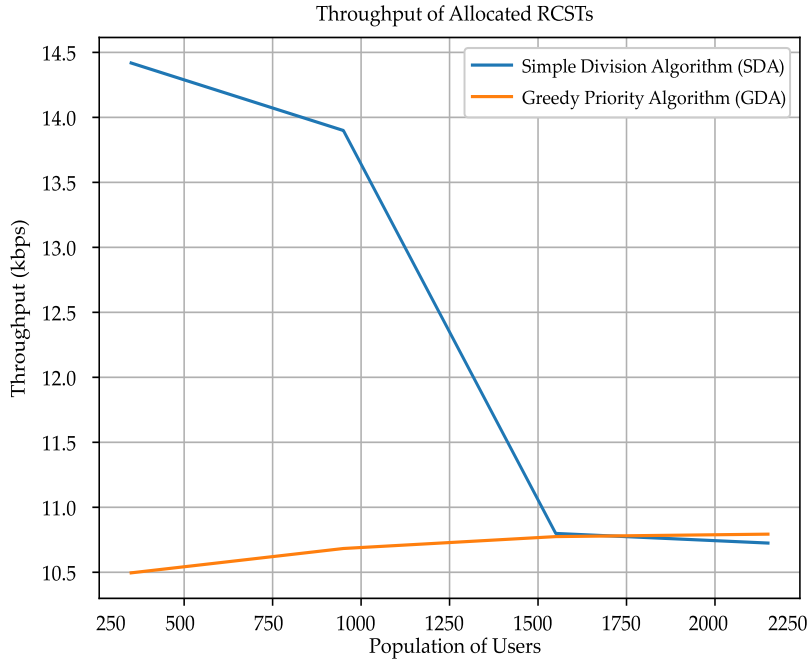

Figure 16 – Average throughput per user of each allocation algorithm for different load points.

One example is shown in Figure 19, which shows the maximum throughput achieved by one user born in the system at specific latitude and longitude coordinates. The start location of the RCST was generated using a probability density function that considers the population density in the region of interest. It is possible to verify that the SDA algorithm provided maximum throughput in regions with higher G/T by following the G/T footprint depicted in Figure 20. As shown by the results of the link budget procedure, areas with better performance corresponded to regions with larger values of E_s/N_0.

5.1.3 Evaluation of Random Access and Data Channel Bandwidths

According to the RCST life cycle diagram in Figure 9, every RCST that attempted to enter the system needed to request an access channel (RA). It was of practical interest to set the best proportion of both pools, RA and DA, to maximize the overall system spectral efficiency. We fixed the total system bandwidth for the comparisons performed here, but the bandwidth values assigned to RA and DA pools were different, each bandwidth distribution was chosen to illustrate different logon behaviors, depicted in Table 6.

In order for the results from Figures 21, 22, and 23 to be understood, they must be analyzed together. Considering the values of Table 6, Scenario A had the

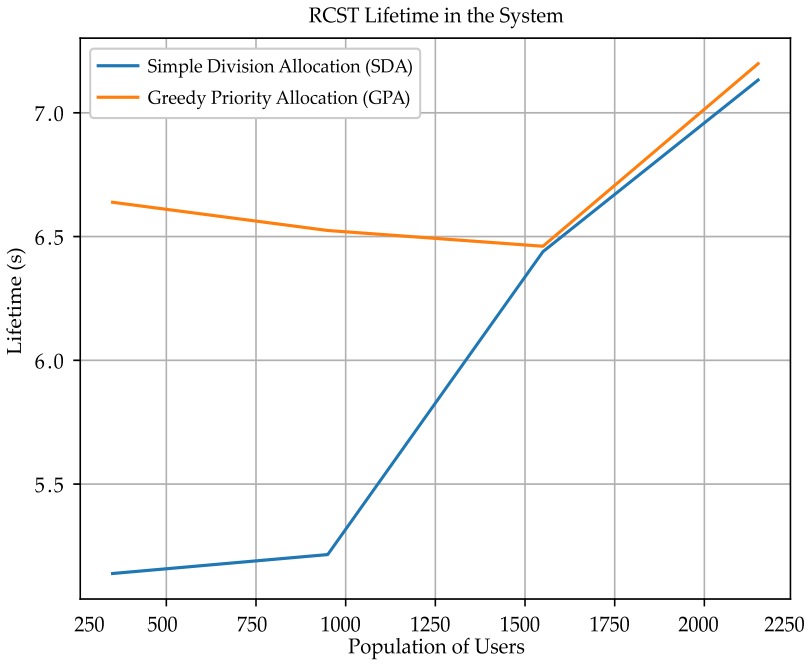

Figure 17 – Average lifetime in seconds of completed users of each allocation algorithm for each load point.

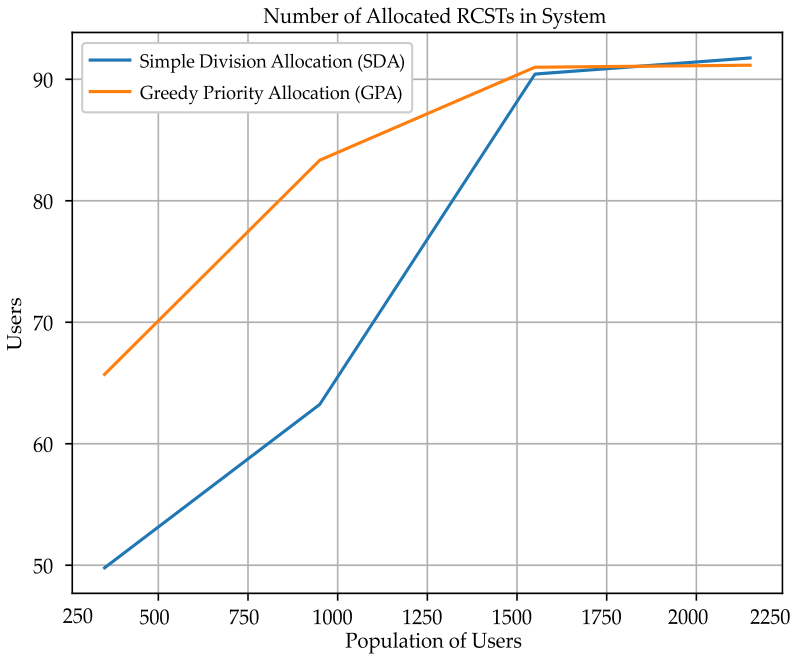

Figure 18 – Behavior of the mean number of simultaneous active users for different load points.

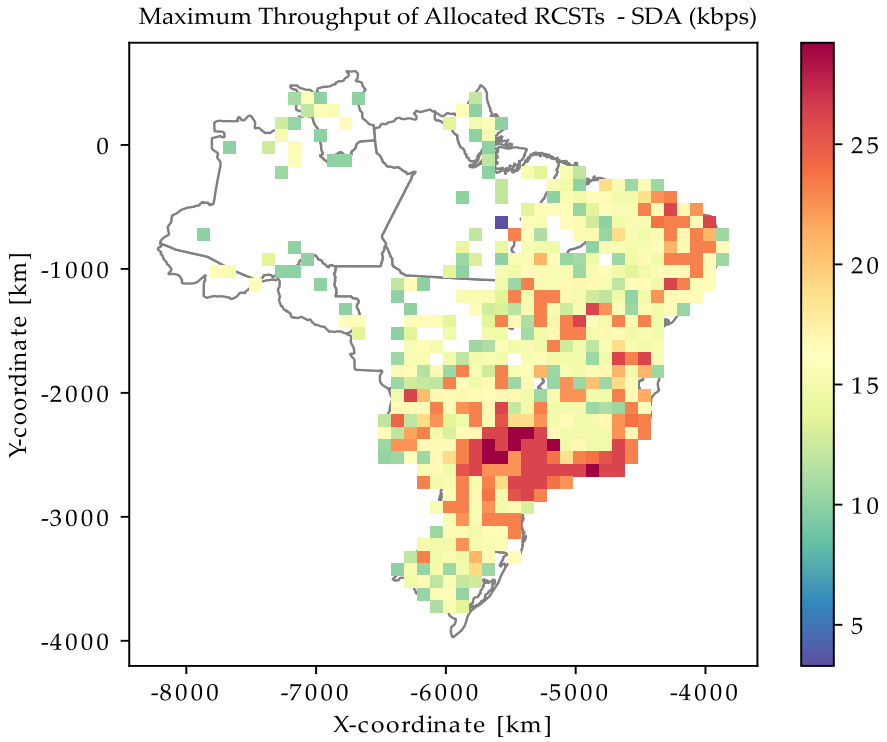

Figure 19 – Heat map of maximum RCST data throughput under the selected coverage area using the SDA algorithm.

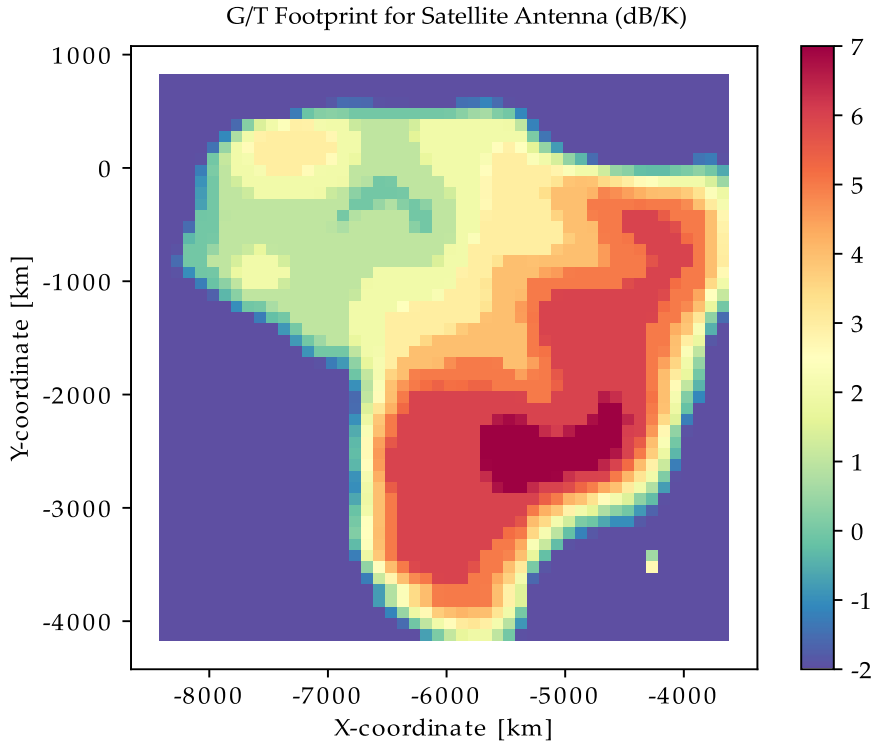

Figure 20 – Heat map of G/T for a GEO satellite, used as a parameter to obtain spatial information of system performance.

Table 6 – Scenarios for analysis of bandwidth allocated to RA and DA resource pools.

Scenario	BW RA (kHz)	BW Data (kHz)
A	150	1350
B	300	1200
C	450	1050

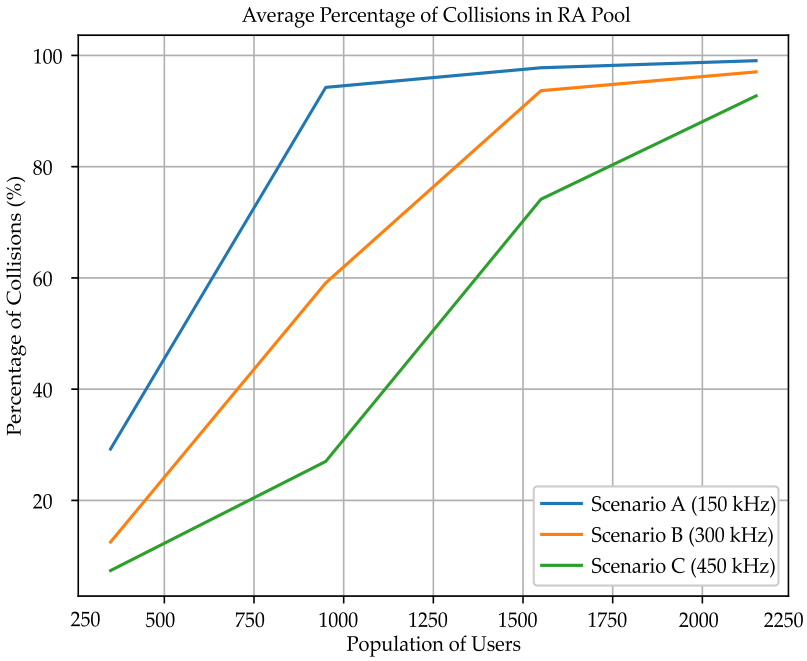

Figure 21 – Average percentage of collisions in the RA frames for different proportions of RA and DA pools. In all cases, the system has the same total bandwidth.

lowest level of resources assigned to the RA pool; as a result, it had the highest collision rate at every load point, as shown in Figure 21. When the system had more collisions, it increased the queue of users attempting to enter the system, and fewer users entered as allocated users. The consequence of the high collision rate , as shown in Figure 22, was that system A had the lowest number of active users at any load point, despite having a higher number of channels to be used in allocation. Thus, theoretically, Scenario A could handle more users, but those users never entered the system because of the collision in the request to transmit. Scenario B started to decrease at a user load point of 1500 for the same reason because the collision rate was above 90%. Scenario C reached this decrease at 2000 users for the same reason. Therefore, the number of BTU in random access area needs to be optimized by the arrival rate of the new users in order to avoid this high collision rate. The expected behavior of the system without the high collision rate is shown in Figure 18. The

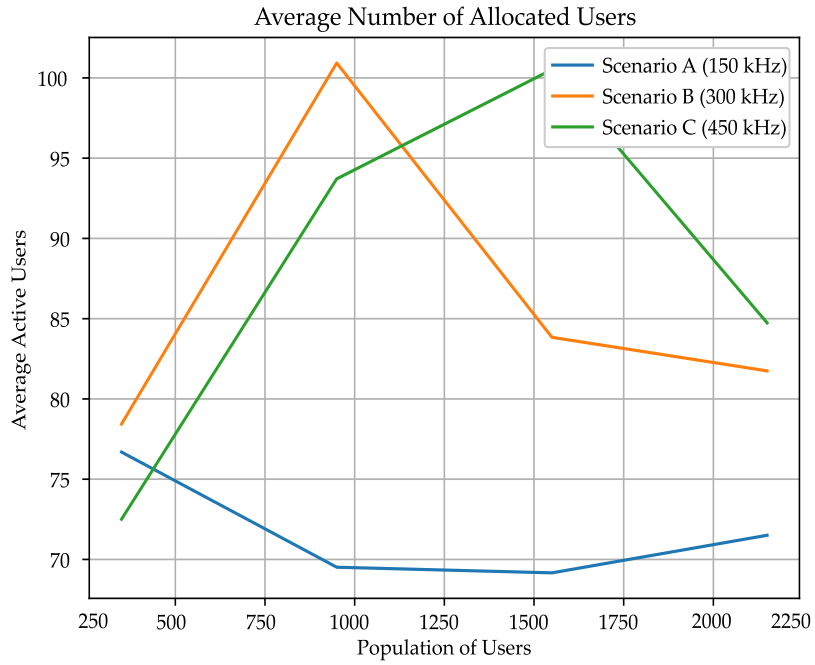

Figure 22 – Average number of active users in the system affected by the collision rates shown in Figure 21.

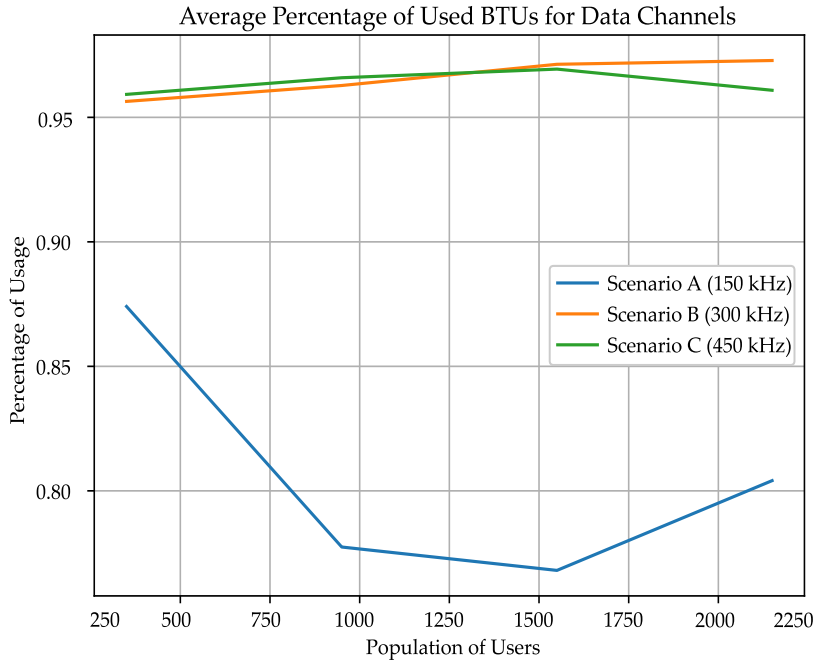

Figure 23 – Average percentage of BTU usage for different proportions of RA and DA pools using the same scenarios as Figures 21 and 22.

correlation between the population density and the G/T footprint is a consequence of the real satellite footprint input file used.

Figure 23 shows how Scenario A could handle more users if more users had been allowed to enter the system, as more than 10% of the BTU resources were unused. This could have been related to the allocation algorithm, but that was not the case in this scenario. There were fewer users of user in this system because those users could never be allocated in the system, due to the collision rate always being above 80% after the 750 load point. These results are not affected by the SDA and GPA allocation because collisions happen during the random access phase, before the RCSTs become active and enter in the green area of the life cycle depicted in Figure 9.

5.2 Game Theory Allocation Scenario Description

The simulator utilizes geospatial data to calculate a detailed link budget for each RCST, using a satellite G/T footprint map as an input parameter. For each traffic load point, a number of N_d simulations, or drops, is performed to obtain statistics of all measurements. For each simulation drop, the RCSTs are randomly distributed in a map, where, for the intents of this paper, we chose the country of Brazil as the benchmarking location. Each point in the map has a birth probability of receiving a new RCST, proportional to the population density of this specific area. This is used to simulate the contrast between high-density populated areas and less populated areas, with different satellite G/T values.

To solve the convex optimization problem defined by the Nash bargaining solution, we used the library CVXPY [75]. For comparison purposes, we implemented a reference scheduler to allocate the BTUs using the traditional game theory allocation algorithm that has all the priorities equal for each RCST. Base results are compared with the new algorithm described previously, in which the BTU allocation is weighted by the p_i parameter, inversely proportional to the information payload per BTU q_i.

All the necessary parameters to replicate the experiment are available in table 7. The simulation ends after $T_{\text{sim}} = 100$ SFs, where the average total number of RCSTs served in a drop is $N_{\text{served}} = \lambda T_{\text{sim}}$, serving ≈ 5.000 RCTs at the last λ simulation point.

5.3 Game Theory Allocation Simulation Results

In Figure 24 we present a comparison of the performance of the legacy game theory algorithm compared to our new proposed game theory algorithm, using as a

Table 7 – Table of simulation parameters.

Parameter	Description	Value
T_{sim}	simulation time in SFs	100
T_{SF}	Time of an SF in BTUs	462
N_{SF}	Number of BTUs in an SF	2772
μ	α distribution mean parameter	2
σ	α distribution std. dev. parameter	0.5
T_{BTU}	Number of symbols in a BTU	270
d_{min}	Min. acceptable data rate for an RCST	10 kbps
N_d	Number of simulation drops	10
V_i	Volume of data for an RCST to transmit	35 kbps

metric the Jain fairness index. It is possible to verify that the proposed algorithm demonstrates an enhancement both in the average Jain index value, reaching a 5% gain at its peak (averaged among all SFs) and a 73% decrease in standard deviation, meaning a more stable and optimized solution. In all load cases, results were closer to the theoretical maximum of 1.

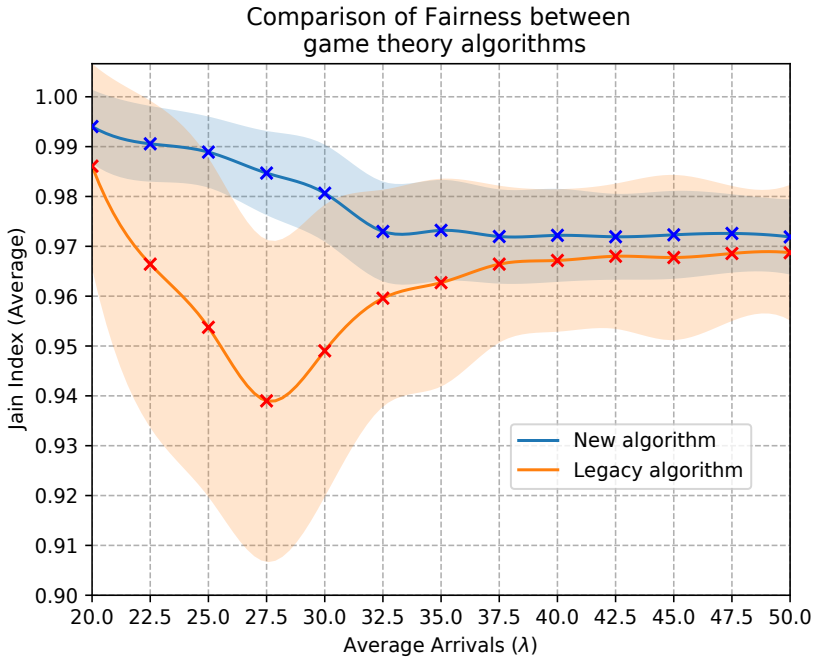

Figure 24 – Fairness performance comparison between game theory algorithms.

The simulation has a larger difference in the domain interval $22.5\lambda \sim 35.0$ λ, a range in which the scheduler strategy shows effectiveness. For low values of λ, the MF-TDMA grid has enough resources to distribute among all RCSTs. The

queue is under-saturated, and the scheduler is able to allocate all the SF resources. The allocation vector $\boldsymbol{\phi}$ reaches maximum fairness, as each RCST receives exactly the amount of BTUs that it expects. On the other hand, when the queue is over-saturated with high values of load, the scheduler can only allocate the minimum value d_i to each RCST in the order of arrival. In this case, there is no space for different allocation strategies to be effective, explaining the asymptotic graph behavior after the 37.5 λ mark in both graphs. Between the extreme cases, we can verify the benefits of using the proposed algorithm.

Beyond the analysis of Jain's index, we also directly evaluated the normalized BTU distribution $\hat{\phi}_i$ obtained for each algorithm. At Figure 25, each point is the average $\hat{\phi}_i$ value among all RCSTs. The maximum value falls in the same load range of Figure 24, with an improvement of $\approx 12.5\%$ in the 30λ mark. This gain appears as the priority for the new algorithm weights the value of a BTU differently for each RCSTs, based on its spectral efficiency, equalizing the distribution between terminals with poor link quality and terminals with high link quality. This result sheds light to Q2 proposed in Section 1.4.

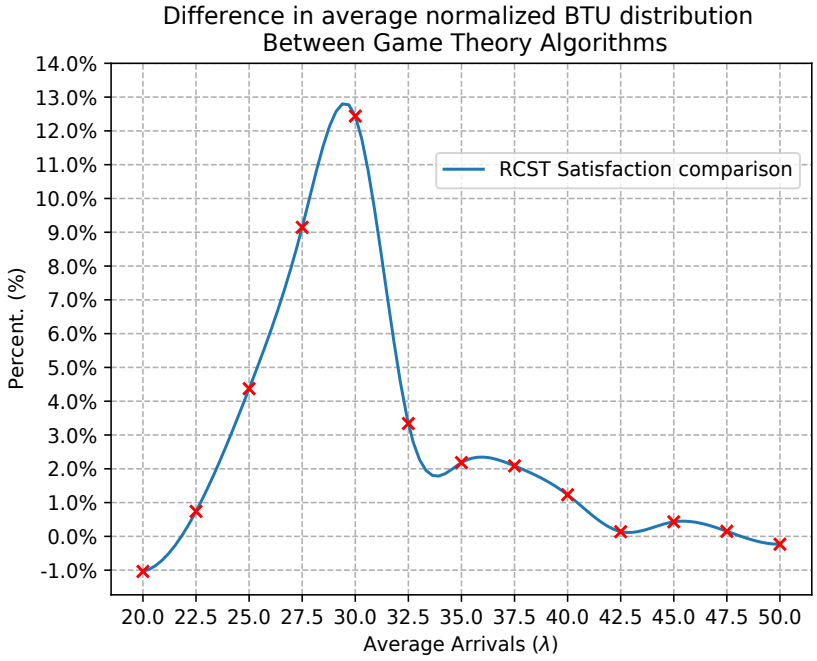

Figure 25 – Difference in average normalized BTU distribution between legacy and proposed algorithm.

5.4 Proposed Queue System Results Analysis

We measured and summarized in some main graphs the queue metrics defined in Section 4.4, that we will readily interpret, comparing our first hypothesis with the conclusion we can draw from the data.

We designed the ρ definition to closely match with the ρ usual definition for general queueing systems, i.e., the traffic intensity. The metric ρ represents the average capacity demand entry over the total capacity of the system. It is important for this definition to not depend on the scheduling algorithm. The designed ρ is invariant to algorithm decision because the SF resource capacity depends only on its spatial dimensions and the average resource demand of BTUs depends only on the RCSTs distribution. This is demonstrated by the result from Figure 26, that is one of the evidences that the ρ defined for our queue model may be appropriate to be assumed as (or at least closely approximate) a general ρ analogy for the queue system, otherwise this constant behavior would not match our expectation.

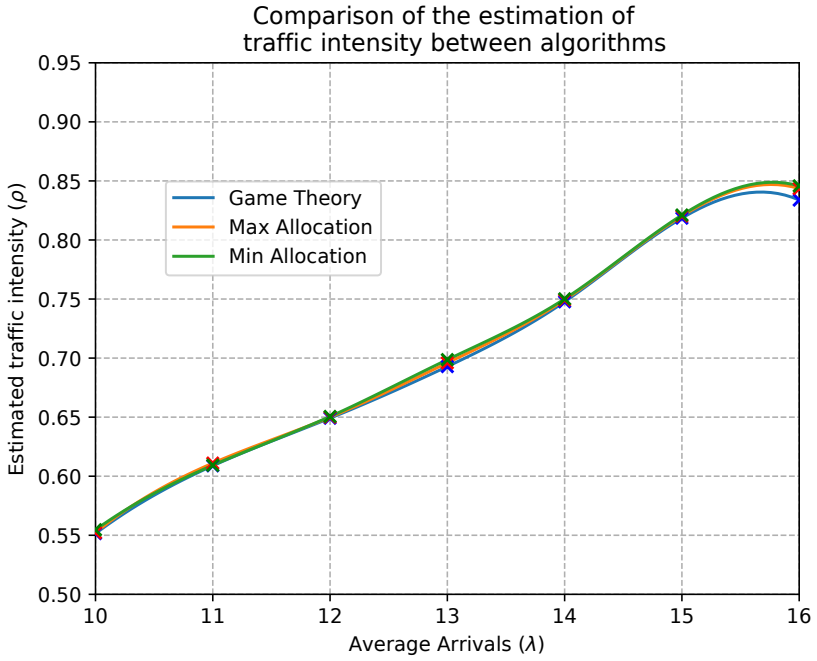

Figure 26 – Measure ρ value for different allocation algorithms.

The m value on the other hand, is affected by the average service rate μ, so it must necessarily change with different allocation policies; in fact, as it was designed to do, this value approximately predicts the maximum allocation capacity of RCSTS on the SF. Result from Figure 27 shows that as the SF gets closer to its capacity and the traffic intensity rises, the number of average allocated RCSTs approaches

asymptotically the predicted m value. The precision of the prediction depends on the allocation demand μ and its standard deviation, represented in Figure 27 by the blue and red bands. We also observe that in the *Min Allocation*, as it has a smaller μ it can allocate more RCSTs than the *Max allocation* algorithm. This has a trade-off in the average throughput per RCST, as we see in Figure 33. Because the *Min Allocation* has a larger standard deviation, the m value predicts the RCST capacity incorrectly by about 5 RCSTs. In the *Max Allocation* Algorithm, having a larger μ and a smaller deviation, we get an error prediction close to zero.

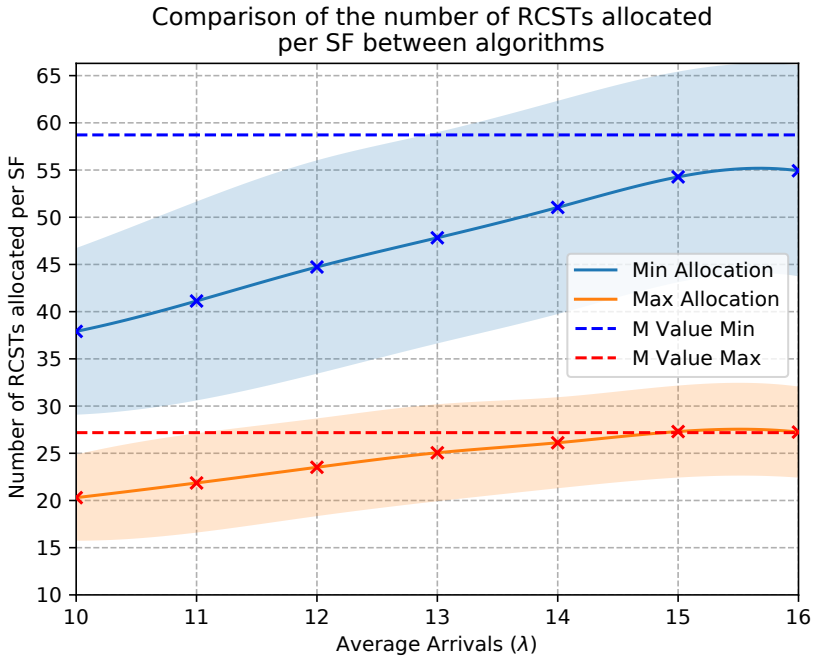

Figure 27 – Average RCSTS allocated per SF comparison between *Max allocation* and *Min Allocation* algorithms and its respective m value predictions.

In the analytical solution for a continuous time $M/M/m$ queue we have that the mean number of costumers in the system is defined by an equation $N = m\rho + R(\rho)$, where $R(\rho)$ is a remainder term that goes to infinity as $\rho \to 1$. We observe this similar behavior of linear proportionality to $m\rho$ in our discrete time m-variant approximation also, Figure 28 demonstrates the close relationship of the measured value of the mean number of RCSTs allocated in the SF and this value predicted using $N_{\text{approx}} = m\rho$.

As discussed in section 4.4, although the ρ value does not depend on the choice of algorithm policy, the average time-until-served for a given RCST do depend on the average service μ, as Figure 29 shows. Notice that in terms of time-until-served, the game theory algorithm tends to have an upper/lower bound relationship

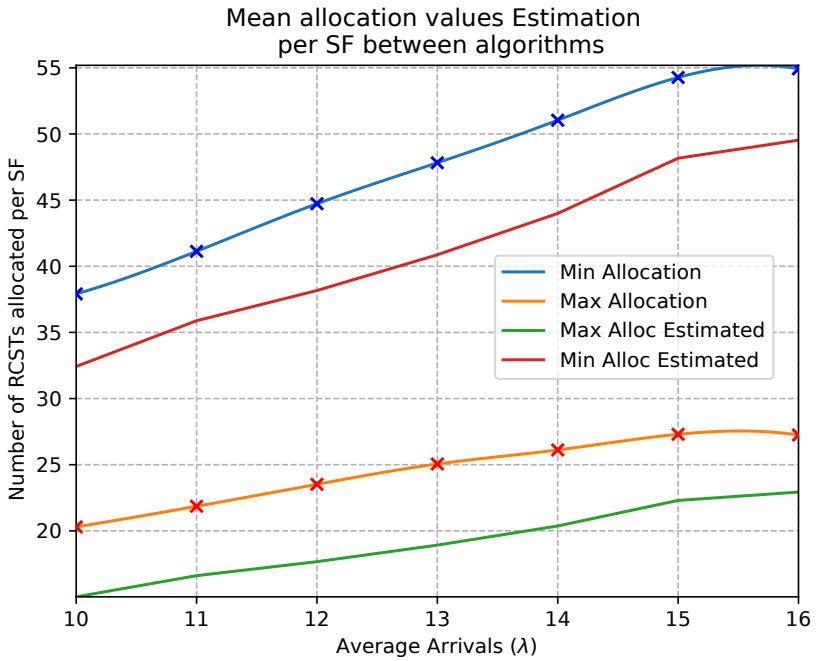

Figure 28 – Comparison between predicted and measured mean allocated RCSTs per SF.

with the *Max/Min allocation* algorithms. We observed that this tendency is preserved throughout the other queue metrics as well.

In the specific case of the time-until-served, when the queue is less saturated, the game theory algorithm tends to allocate the maximum possible capacity to the RCST, coinciding with the *Max allocation* algorithm. This behavior inverts when the queue saturates, as the game theory algorithm tends to allocate the minimum possible capacity to an RCST. There is an outlier case point $\lambda = 16$, where this upper bound/lower bound expectation is not met. The explanation for this phenomenon can be attributed to the sample size of SFs and the transient behavior of the queue at the beginning of the simulation. When the queue is not yet in the steady state condition, the game theory algorithm behaves more frequently as the *Max allocation* algorithm, having a significant impact lowering the time-until-served.

We measured the average queue size of the three allocation algorithms, that we show in Figure 30. As expected by Little's law, the *Max Allocation* algorithm has the largest queue size because it has the largest waiting time; for the same reason, the *Min allocation* has the smallest waiting time. The game theory allocation algorithm shows a behavior that diverges from Little's law, this is due to the non-stochastic nature of its allocation policy. As the game theory algorithm tries to optimize the resource capacity allocation, it modifies the μ value dynamically and changes the

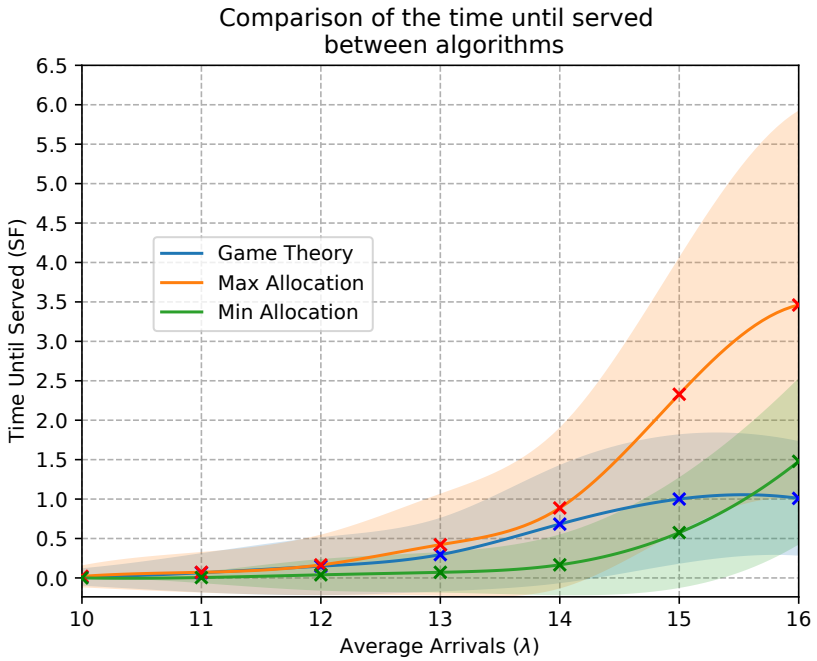

Figure 29 – Measured time until served for different resource allocation algorithms.

average number of servers m average in this process, diminishing the queue size and making the queue process non-stationary, contradicting one of the assumptions of Little's law.

The average completion time for a given number of RCSTs depends only on the capacity available in the SF, not on the allocation policy, so the two major trade-offs are the waiting time of a RCST and its average throughput. We see in Figure 29 and in Figure 33 that although the *Max allocation* algorithm has a larger waiting time, it also has a larger average throughput, a consequence of this observation.

We see in Figure 31 the curve fitting of the time until served simulated, we used the Markov Chain model of the MF-TDMA queue system defined in section 4.4. We see some of the α values used in the total simulation, 28 different α values were used, which ranged from 1.0 to 3.7 with 0.1 steps. The coefficients are fed into the GTAC algorithm, it searches for the maximal α value to a given ρ that do not cross the predetermined waiting time threshold.

We see in Figure 32 the waiting time response of the GTAC algorithm, noticing that it meets the threshold of 1 SF waiting time with some ripples, that can be attributed to the time dynamic behavior of the simple proportional control system defined for the allocation policy. This result, combined with Figure 33 where we observe that the average throughput of the GTAC algorithm is closer to the *Max*

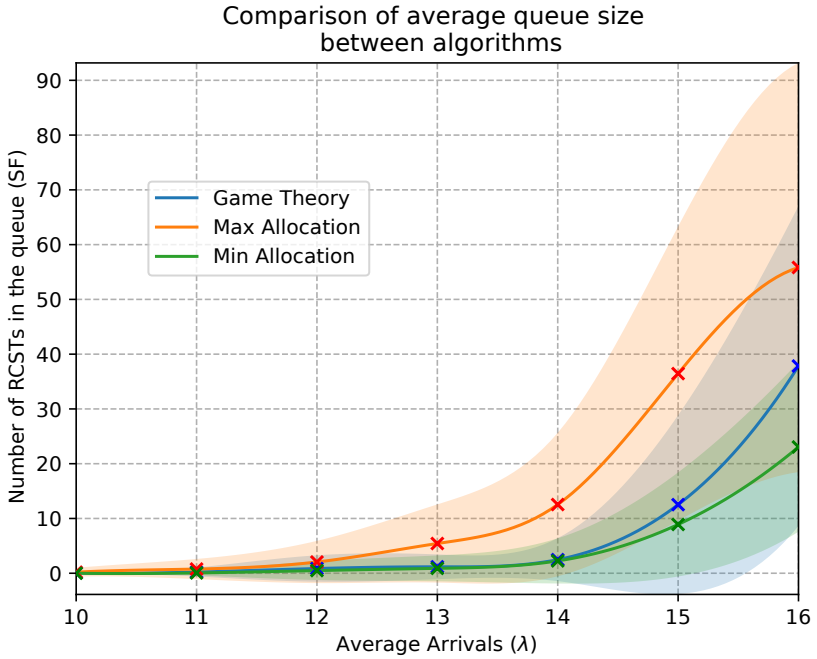

Figure 30 – Comparison of average Number of RCSTs waiting to be served in the queue between algorithms.

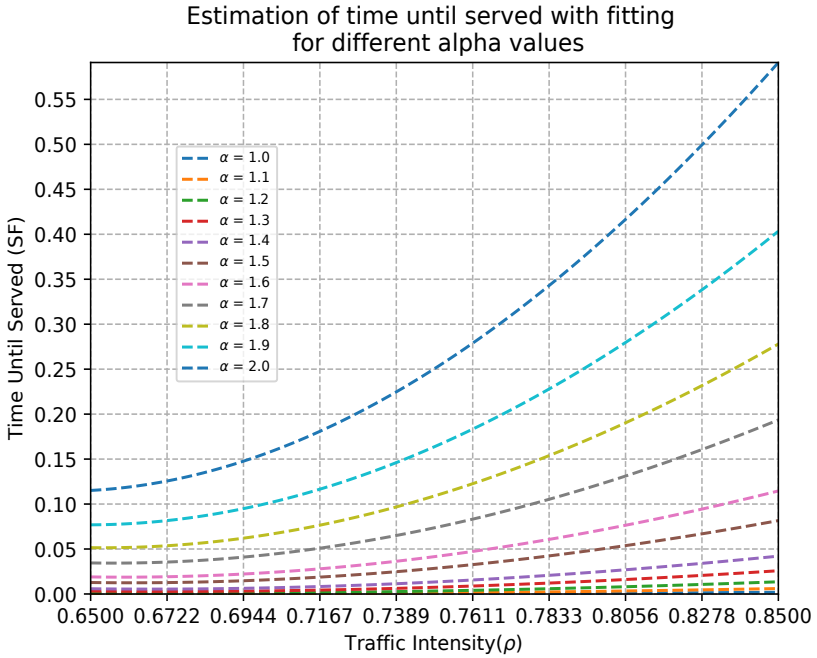

Figure 31 – Time until served curve fitting for different alpha values.

allocation throughput, shows that the GTAC algorithm met its purpose of balancing the trade-off between waiting time and average throughput. We kept the capacity transmission latency below a threshold, which is useful for time-sensitive applications, while maintaining a higher throughput and ensuring better QoS. The results found in this section coupled with the system modeling shows a partial affirmative to Q3 proposed in Section 1.4.

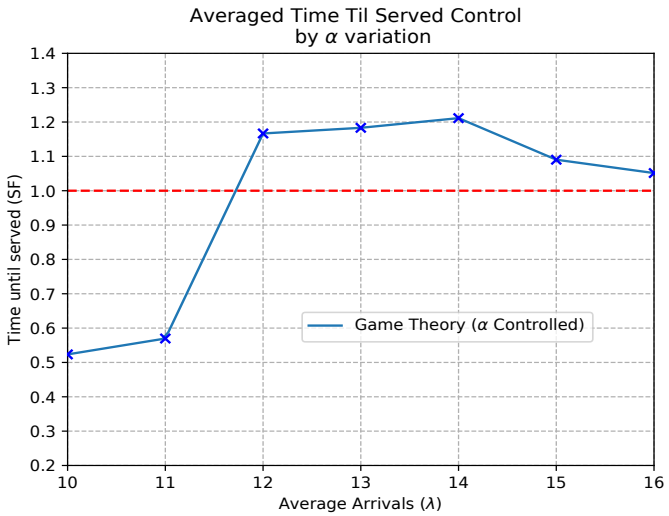

Figure 32 – Time until served measured in the GTAC algorithm

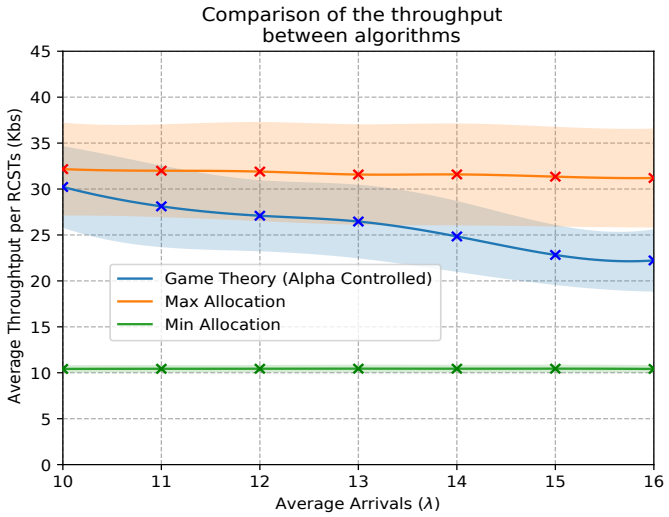

Figure 33 – Comparison between average throughput per SF between resource allocation algorithms.

CHAPTER 6

CONCLUSION AND FUTURE WORK

6.1 Discussion and Conclusion

In conclusion, this work presented an event-driven, system-level simulator with implementation details for the PHY and MAC layers compliant with the DVB-RCS2 ETSI standard. We provided three use case examples for the proposed simulation framework in order to help evaluate and design a GEO satellite system with a large coverage area within a realistic scenario. This proposed framework shows two allocation strategies, and can be used in the future to test and evaluate new allocation strategies. Additionally, the output was georeferenced and plotted on the map of the scenario. Finally, the collision detection mechanism showed how this could affect the performance of the whole system. The framework is also capable of providing an extensive set of results and KPIs, such as packet loss rate (PLR). Performance of other receivers will be presented in future works and an extension of the code to handle LEO trajectories is currently under development. We focused on the behavior and analysis of DVB-RCS2. Optimization of the code is a topic of future research, as well as an evaluation of the performance and code complexity.

In addition, we also proposed a modification to the traditional game theory framework for capacity resource allocation in a DVB-RCS2 MF-TDMA SF, considering the information payload q_i on each waveform ID to weigh the priority parameters in the convex optimization problem that arises from the Nash bargaining solution. The new procedure achieved better performance when compared to the traditional formulation, suggesting its employment in new scenarios. As we delve further into the resource allocation problem, we defined a queuing model for the MF-TDMA scheduling system using request-based non-priority allocation schemes. This model allowed for the numerical prediction of some key metrics, such as the maximum average allocated RCSTs at each SF iteration, the average number of RCSTs allocated per SF and a metric that predicts the traffic intensity of the system. Using the queue model, we can predict when the queue saturates and determine a Markov chain model numerical solution for the average time until served for each RCST. This allows the definition of the GTAC algorithm and a scheduling policy that maintains the

time until served at a threshold while maximizing throughput per SF.

6.2 Future Work

A first possible extension to this work is to apply the same priority strategy to multi-beam satellites, where a second priority would be assigned to each beam. A second possibility is the investigation of scenarios with larger SF lengths to accommodate a massive number of users (in the order of 10^6) with low traffic density for ultra-reliable communications where the high latency of the GEO satellite link is not a problem. Another possibility is the insertion of LEO orbits in the simulator to take into account the Doppler effect and verify the algorithm's behavior in a dynamic SINR environment, it is necessary to compare the performance of our defined framework with other simulators.

As the probability distributions for both the arrivals and the completions at each state were implemented and idealized based on typical assumptions, it is always possible to improve the model performance by gathering real data for these probability distributions, we can always run longer simulations, and keep track of these metrics with more precision. Another possibility that was not explored in this paper, is to try and solve the Markov Chain model defined here analytically using the Z-transform, as this is commonly done for more simple queues such as the unique server discrete time queue. Although there were trials of solving such systems in closed form, the equations get unpractical very quickly as queue systems grow in complexity, so we chose to focus on numerical analysis to not run out of scope for the simulator validation.

Another possibility for future work is the analysis of periodic behavior in the queue. As our system identifies an RCSTs as a terminal that completes a task and logs out of the system, we might, in an extension, interpret the RCSTs as periodic customers of the MF-TDMA queue. That way, we can, in the long run, consider using the user task distribution to define a better policy to encompass an improvement to the whole allocation system.

Finally, for the GTAC algorithm, there is room to explore the time dependent control of the queue system. The GTAC algorithm does a linear proportional feedback to control the allocation, so we see the oscillations of the prediction-controlling dynamic in the graphs. This might be improved with the use of more sophisticated control theory techniques.

BIBLIOGRAPHY

[1] ITU-D. *ITU Telecommunication Development Sector Statistics*. URL: <https://www.itu.int/en/ITU-D/Statistics/Pages/stat/default.aspx>. (Accessed: 03.Aug.2020).

[2] Ericsson Mobility Report. *IoT connections outlook*. URL: <https://www.ericsson.com/en/mobility-report/reports/june-2020/iot-connections-outlook>. (Accessed: 05.Aug.2020).

[3] *ETSI GMR-1 3G 41.202 - TS 101 376-1-3 V3.1.1 (2009-07): GEO-Mobile Radio Interface Specifications (Release 3); Third Generation Satellite Packet Radio Service; Part 1: General specifications; Sub-part 3: General System Description*. 2009.

[4] P. Wang et al. "Convergence of Satellite and Terrestrial Networks: A Comprehensive Survey". In: *IEEE Access* 8 (2020), pp. 5550–5588.

[5] ETSI EN 302 307-2. "Digital Video Broadcasting (DVB);Second generation framing structure, channel coding and modulation systems for Broadcasting, Interactive Services, News Gathering and other broadband satellite applications; Part 2: DVB-S2 Extensions (DVB-S2X)," in: 2020.

[6] ETSI EN 301 545-2. "Digital video broadcasting (DVB); second generation DVB interactive satellite system (DVB-RCS2); part 2: lower layers for satellite standard," in: 2014.

[7] ETSI EN 301 545-4. "Digital video broadcasting (DVB); second generation DVB interactive satellite system (DVB-RCS2); part 4: guidelines for implementation and use of EN 301 545-2," in: 2014.

[8] Ying Wang, Jing Xu, and Lisi Jiang. "Challenges of System-Level Simulations and Performance Evaluation for 5G Wireless Networks". In: *IEEE Access* 2 (2014), pp. 1553–1561. DOI: <10.1109/ACCESS.2014.2383833>.

[9] Anand Nayyar and Rajeshwar Singh. "A Comprehensive Review of Simulation Tools for Wireless Sensor Networks (WSNs)". In: (Jan. 2015), pp. 19–47. DOI: <10.5923/j.jwnc.20150501.03>.

[10] D.P. Connors, Bo Ryu, and Son Dao. "Modeling and simulation of broadband satellite networks .I. medium access control for QoS provisioning". In: *IEEE Communications Magazine* 37.3 (1999), pp. 72–79. DOI: <10.1109/35.751498>.

[11] Jani Puttonen et al. "Satellite Model for Network Simulator 3". In: ICST, Aug. 2014. DOI: <10.4108/icst.simutools.2014.254631>.

[12] Jani Puttonen, Lauri Sormunen, and Janne Kurjenniemi. "Radio resource management in DVB-RCS2 satellite systems". In: *34th AIAA International Communications Satellite Systems Conference, 2016* October (2016), pp. 18–20. DOI: <10.2514/6.2016-5734>. URL: <https://doi.org/10.2514/6.2016-5734>.

[13] Dong-Hyun Jung, Min-Su Shin, and Joon-Gyu Ryu. "Fairness-Based Superframe Design and Resource Allocation for Dynamic Rate Adaptation in DVB-RCS2 Satellite Systems". In: *IEEE Communications Letters* PP.2 (2019), pp. 1–1. ISSN: 1089-7798. DOI: <10.1109/lcomm.2019.2928288>.

[14] J. R. Bejarano, C. Miguel Nieto, and F. J. Ruiz Piñar. "MF-TDMA Scheduling Algorithm for Multi-Spot Beam Satellite Systems Based on Co-Channel Interference Evaluation". In: *IEEE Access* 7 (2019), pp. 4391–4399.

[15] E. Casini, R. De Gaudenzi, and O. Del Rio Herrero. "Contention Resolution Diversity Slotted ALOHA (CRDSA): An Enhanced Random Access Schemefor Satellite Access Packet Networks". In: *IEEE Transactions on Wireless Communications* 6.4 (2007), pp. 1408–1419.

[16] Antonio Pietrabissa and Andrea Fiaschetti. "Dynamic uplink frame optimization with adaptive coding and modulation in DVB-RCS2 satellite networks". In: *International Journal of Satellite Communications and Networking* 31.3 (2013), pp. 123–139. DOI: <10.1002/sat.1024>.

[17] W. Li, R. Mani, and P. J. Mosterman. "Extensible Discrete-Event Simulation framework in SimEvents". In: *2016 Winter Simulation Conference (WSC)*. 2016, pp. 943–954. DOI: <10.1109/WSC.2016.7822155>.

[18] Yue Zhang et al. "A Discrete-Event and Hybrid Simulation Framework Based on SimEvents for Intelligent Transportation System Analysis". In: *IFAC-PapersOnLine* 51.7 (Jan. 2018), pp. 323–328. ISSN: 24058963. DOI: <10.1016/j.ifacol.2018.06.320>.

[19] *Sharing studies between IMT-2020 and the radio astronomy service in the 42.5-43.5 GHz ban*. Working Draft Proposed Standard. Brazil, 2018.

[20] *SimPy Documentation*. <https://simpy.readthedocs.io/en/latest/>.

[21] Jean-Baptiste Dupé. *Ordonnancement et gestion des ressources pour un système de télécommunications haut débit : Optimisation de la bande passante satellite*. Oct. 2015.

[22] Yang Hong et al. "Optimal power allocation for multiple beam satellite systems". In: Feb. 2008, pp. 823–826. DOI: <10.1109/RWS.2008.4463619>.

[23] Antoni Morell, Gonzalo Seco-Granados, and Angeles Vazquez-Castro. "SAT03-3: Joint Time Slot Optimization and Fair Bandwidth Allocation for DVB-RCS Systems". In: Jan. 2007, pp. 1–5. DOI: <10.1109/GLOCOM.2006.517>.

[24] Gonzalo Seco-Granados et al. "Algorithm for Fair Bandwidth Allocation with QoS Constraints in DVB-S2/RCS." In: Jan. 2006.

[25] T. Zhang, Q. Dong, and J. Zhang. "MF-TDMA Optimal Timeslot Allocation Algorithm". In: *2008 China-Japan Joint Microwave Conference*. 2008, pp. 824–828.

[26] S. Alouf et al. "Quasi-optimal bandwidth allocation for multi-spot MFTDMA satellites". In: *Proceedings IEEE 24th Annual Joint Conference of the IEEE Computer and Communications Societies.* Vol. 1. 2005, 560–571 vol. 1.

[27] Li Hui and Tao Yang. "Queues with a variable number of servers". In: *European Journal of Operational Research* 124 (Feb. 2000), pp. 615–628. DOI: <10.1016/S0377-2217(99)00175-7>.

[28] Herwig Bruneel and Ilse Wuyts. "Analysis of discrete-time multiserver queueing models with constant service times". In: *Operations Research Letters* 15.5 (1994), pp. 231–236. ISSN: 0167-6377. DOI: <https://doi.org/10.1016/0167-6377(94)90082-5>. URL: <https://www.sciencedirect.com/science/article/pii/0167637794900825>.

[29] Peixia Gao, Sabine Wittevrongel, and Herwig Bruneel. "Discrete-time multiserver queues with geometric service times". In: *Computers Operations Research* 31.1 (2004), pp. 81–99. ISSN: 0305-0548. DOI: <https://doi.org/10.1016/S0305-0548(02)00155-7>. URL: <https://www.sciencedirect.com/science/article/pii/S0305054802001557>.

[30] Peixia Gao, Sabine Wittevrongel, and Herwig Bruneel. "Analysis of discrete-time multiserver queues with constant service times and correlated arrivals". In: (Jan. 2005).

[31] Jani Puttonen et al. "Satellite model for network simulator 3". In: *SIMUTools 2014 - 7th International Conference on Simulation Tools and Techniques* (2014), pp. 86–91. DOI: <10.4108/icst.simutools.2014.254631>.

[32] Vincent Boussemart Brandt and Hartmut. "A tool for satellite communications Advanced DVB-RCS / DVB-S2 system and protocol simulator". In: *2008 10th International Workshop on Signal Processing for Space Communications* (2008), pp. 1–5.

[33] V. Boussemart and H. Brandt. "a System Simulator for Advanced Dvb-S2 / Rcs Multibeam Systems". In: *Deutscher Luft- und Raumfahrtkongress* (2008).

[34] R. A. R. Fischer and J. P. Leite. "DVB-RCS2 Satellite Standard Performance Assessment Through a Link-Level Python Simulator". In: *38th Brazilian Symposium of Telecommunications - SBrT, Florianópolis, Brazil*. Nov. 2020, pp. 1–2.

[35] Anatel. *[319] Sharing studies between IMT-2020 and the radio astronomy service in the 42.5-43.5 GHz band*. 2018. URL: <https://www.itu.int/md/R15-TG5.1-C-0319/_page.print>.

[36] Anatel. *On the convergence of Monte-Carlo approach for sharing and compatibility studies between IMT-2020 and other services*. Tech. rep. 2018. URL: <https://www.itu.int/md/R15-TG5.1.AR-C-0241/fr>.

[37] George F. Riley and Thomas R. Henderson. "The *ns-3* Network Simulator". In: *Modeling and Tools for Network Simulation*. Ed. by Klaus Wehrle, Mesut Günes, and James Gross. Springer, 2010, pp. 15–34. DOI: <10.1007/978-3-642-12331-3_2>. URL: <https://doi.org/10.1007/978-3-642-12331-3%5C_2>.

[38] András Varga. "The OMNET++ discrete event simulation system". In: *Proc. ESM'2001* 9 (Jan. 2001).

[39] Anatel. *SHARC, simulator for use in SHARing and Compatibility studies of radiocommunication systems*. 2018. URL: <https://github.com/SIMULATOR-WG/SHARC>.

[40] Virgil Labrador. *Satellite communication - Satellite applications | Britannica*. 2019. URL: <https://www.britannica.com/technology/satellite-communication/Satellite-applications> (visited on 11/16/2021).

[41] *Engineering and Technology History Wiki*. URL: <https://ethw.org/Communications_Satellites> (visited on 11/16/2021).

[42] Oltjon Kodheli et al. "Satellite Communications in the New Space Era: A Survey and Future Challenges". In: *IEEE Communications Surveys Tutorials* 23.1 (2021), pp. 70–109. DOI: <10.1109/COMST.2020.3028247>.

[43] ITU. "Recommendation ITU-R V.431-8: Nomenclature of the frequency and wavelength bands used in telecommunications". In: (2015).

[44] ETSI. "Recommendation ITU-R P.676-12 - Attenuation by atmospheric gases and related effects". In: 1 (2019).

[45] Koen Willems. "Business Insight on DVB-S2X DVB-S2X DEMYSTIFIED". In: (2014). URL: <www.newtec.eu>.

[46] M. A. V. Castro, L. S. Ronga, and M. Werner. "Dynamic Rate Adaptation (DRA) and Adaptive Coding and Modulation (ACM) efficiency comparison for a DVB-RCS system". In: *2005 2nd International Symposium on Wireless Communication Systems*. 2005, pp. 822–826.

[47] M. Angelone et al. "Performance of a combined dynamic rate adaptation and adaptive coding modulation technique for a DVB-RCS2 system". In: *2012 6th Advanced Satellite Multimedia Systems Conference (ASMS) and 12th Signal Processing for Space Communications Workshop (SPSC)*. 2012, pp. 124–131.

[48] ETSI. "Digital Video Broadcasting (DVB); Second Generation DVB Interactive Satellite System (DVB-RCS2); Part 1: Overview and System Level specification". In: 1 (2014), pp. 1–22.

[49] J. von Neumann and O. Morgenstern. *Theory of games and economic behavior*. Princeton University Press, 1947.

[50] Christopher Griffin. "Game Theory: Penn State Math 486 Lecture Notes". In: (2010).

[51] R. Gibbons. *A Primer in Game Theory*. Pearson Education, 1992.

[52] H. Yaiche, R.R. Mazumdar, and C. Rosenberg. "A game theoretic framework for bandwidth allocation and pricing in broadband networks". In: *IEEE/ACM Transactions on Networking* 8.5 (2000), pp. 667–678. DOI: <10.1109/90.879352>.

[53] Zhu Han et al. "Resource Allocation for Multiuser Cooperative OFDM Networks: Who Helps Whom and How to Cooperate". In: *IEEE Transactions on Vehicular Technology* 58.5 (2009), pp. 2378–2391. DOI: <10.1109/TVT.2008.2004267>.

[54] E. Chaput et al. "Utility function based packet scheduling over DVB-S2". In: *2013 IEEE International Conference on Communications (ICC)*. 2013, pp. 4288–4292. DOI: <10.1109/ICC.2013.6655238>.

[55] John Nash. "Two-Person Cooperative Games". In: *Econometrica* 21.1 (1953), pp. 128–140. ISSN: 00129682, 14680262. URL: <http://www.jstor.org/stable/1906951>.

[56] John C. Harsanyi. "Measurement of social power, opportunity costs, and the theory of two-person bargaining games". In: *Behavioral Science* 7.1 (1962), pp. 67–80. DOI: <https://doi.org/10.1002/bs.3830070105>.

[57] Gordon C. Rausser, Johan Swinnen, and Pinhas Zusman. *Political Power and Economic Policy: Theory, Analysis, and Empirical Applications*. Cambridge University Press, 2011. DOI: <10.1017/CBO9780511978661>.

[58] Ehud Kalai and Meir Smorodinsky. "Other Solutions to Nash's Bargaining Problem". In: *Econometrica* 43.3 (1975), pp. 513–518. ISSN: 00129682, 14680262. URL: <http://www.jstor.org/stable/1914280>.

[59] Ehud Kalai. "Proportional Solutions to Bargaining Situations: Interpersonal Utility Comparisons". In: *Econometrica* 45.7 (1977), pp. 1623–1630. ISSN: 00129682, 14680262. URL: <http://www.jstor.org/stable/1913954>.

[60] Daria Terekhov, Douglas G. Down, and J. Christopher Beck. "Queueing-theoretic approaches for dynamic scheduling: A survey". In: *Surveys in Operations Research and Management Science* 19.2 (2014), pp. 105–129. ISSN: 1876-7354. DOI: <https://doi.org/10.1016/j.sorms.2014.09.001>. URL: <https://www.sciencedirect.com/science/article/pii/S1876735414000233>.

[61] Daria Terekhov et al. "Integrating Queueing Theory and Scheduling for Dynamic Scheduling Problems". In: *The Journal of Artificial Intelligence Research (JAIR)* 50 (July 2014). DOI: <10.1613/jair.4278>.

[62] Moshe Zukerman. *Introduction to Queueing Theory and Stochastic Teletraffic Models*. 2021. arXiv: <1307.2968> [math.PR].

[63] Walmes Zeviani. *Walmes Zeviani - Tikz Gallery*. <http://leg.ufpr.br/~walmes/Tikz/>. [Online; accessed 20-Dec-2021].

[64] C.G. Cassandras and Stephane Lafortune. "Introduction to Discrete Event Systems". In: Jan. 2010, p. 800. ISBN: 1441941193. DOI: <10.1007/978-0-387-68612-7>.

[65] *Store Object Documentation*. <https://simpy.readthedocs.io/en/latest/api_reference/simpy.resources.html#simpy.resources.store.Store>.

[66] Raj Jain, Dah Ming Chiu, and Hawe WR. "A Quantitative Measure Of Fairness And Discrimination For Resource Allocation In Shared Computer Systems". In: *CoRR* cs.NI/9809099 (Jan. 1998).

[67] Huaizhou SHI et al. "Fairness in Wireless Networks:Issues, Measures and Challenges". In: *IEEE Communications Surveys Tutorials* 16.1 (2014), pp. 5–24. DOI: <10.1109/SURV.2013.050113.00015>.

[68] Tian Lan et al. “An Axiomatic Theory of Fairness in Network Resource Allocation”. In: *2010 Proceedings IEEE INFOCOM*. 2010, pp. 1–9. DOI: <10.1109/INFCOM.2010.5461911>.

[69] Daniel Palomar and Javier Fonollosa. “Practical algorithms for a family of waterfilling Solutions”. In: *Signal Processing, IEEE Transactions on* 53 (Mar. 2005), pp. 686–695. DOI: <10.1109/TSP.2004.840816>.

[70] Qilin Qi, Andrew Minturn, and Yaoqing Yang. “An efficient water-filling algorithm for power allocation in OFDM-based cognitive radio systems”. In: *2012 International Conference on Systems and Informatics (ICSAI2012)*. 2012, pp. 2069–2073. DOI: <10.1109/ICSAI.2012.6223460>.

[71] P.D. Mitchell, D. Grace, and T.C. Tozer. “Analytical model of round-robin scheduling for a geostationary satellite system”. In: *IEEE Communications Letters* 7.11 (2003), pp. 546–548. DOI: <10.1109/LCOMM.2003.820104>.

[72] *ETSI TS 101 545-1 V1.2.1 - Digital Video Broadcasting (DVB); Second Generation DVB Interactive Satellite System (DVB-RCS2); Part 1: Overview and System Level specification*. 2014.

[73] *ETSI TS 101 545-3 V1.2.1 - Digital Video Broadcasting (DVB); Second Generation DVB Interactive Satellite System (DVB-RCS2); Part 3: Higher Layers Satellite Specification*. 2014.

[74] Nperf. *Coverage Map*. https://www.nperf.com/pt/map/BR/-/-/signal/?ll=-15.126554432601873&lg=-51.64499999999999&zoom=4. May 2019.

[75] *CVXPY Documentation*. <https://www.cvxpy.org>.

Annex

ANNEX A

SPECTRAL EFFIENCY TABLE

Waveform ID (Table A-1 of [i.1])	Burst Size (symbols)	Guard (symbols)	Payload (bits)	Efficiency (Bits/Symbol)	E_s/N_0 @ PER = 10^{-5}
44	266	4	408	1,51	7,3
45	266	4	440	1,63	8,71
46	266	4	496	1,84	10,04
47	266	4	552	2,04	11,59
48	266	4	672	2,49	11,73
49	266	4	744	2,76	13,18
3	536	4	304	0,56	0,22
4	536	4	472	0,87	2,34
5	536	4	680	1,26	4,29
6	536	4	768	1,42	5,36
7	536	4	864	1,60	6,68
8	536	4	920	1,70	8,08
9	536	4	1 040	1,93	9,31
10	536	4	1 152	2,13	10,85
11	536	4	1 400	2,59	11,17
12	536	4	1 552	2,87	12,56
13	1 616	4	984	0,61	-0,51
14	1 616	4	1 504	0,93	1,71
15	1 616	4	2 112	1,30	3,69
16	1 616	4	2 384	1,47	4,73
17	1 616	4	2 664	1,64	5,94
18	1 616	4	2 840	1,75	7,49
19	1 616	4	3 200	1,98	8,77
20	1 616	4	3 552	2,19	10,23
21	1 616	4	4 312	2,66	10,72
22	1 616	4	4 792	2,96	12,04
42	3 236	4	984	0,30	-3,52
43	3 236	4	1 504	0,46	-1,3

Figure 34 – Table with the spectral efficiency information for all linear waveforms in DVB-RCS2/DVB-S2X standard. Adapted from [7, p.179]